

# Association of Lower Rostral Anterior Cingulate GABA+ and Dysregulated Cortisol Stress Response With Altered Functional Connectivity in Young Adults With Lifetime Depression: A Multimodal Imaging Investigation of Trait and State Effects

Maria Ironside, D.Phil., Jessica M. Duda, B.A., Amelia D. Moser, M.A., Laura M. Holsen, Ph.D., Chun S. Zuo, Ph.D., Fei Du, Ph.D., Sarah Perlo, B.S., Christine E. Richards, B.S., Xi Chen, Ph.D., Lisa D. Nickerson, Ph.D., Kaylee E. Null, B.A., Shiba M. Esfand, B.A., Madeline M. Alexander, Ph.D., David J. Crowley, A.L.M., Meghan Lauze, B.S., Madhusmita Misra, M.D., M.P.H., Jill M. Goldstein, Ph.D., Diego A. Pizzagalli, Ph.D.

**Objective:** Preclinical work suggests that excess glucocorticoids and reduced cortical  $\gamma$ -aminobutyric acid (GABA) may affect sex-dependent differences in brain regions implicated in stress regulation and depressive phenotypes. The authors sought to address a critical gap in knowledge, namely, how stress circuitry is functionally affected by glucocorticoids and GABA in current or remitted major depressive disorder (MDD).

**Methods:** Multimodal imaging data were collected from 130 young adults (ages 18–25), of whom 44 had current MDD, 42 had remitted MDD, and 44 were healthy comparison subjects. GABA+ ( $\gamma$ -aminobutyric acid and macromolecules) was assessed using magnetic resonance spectroscopy, and task-related functional MRI data were collected under acute stress and analyzed using data-driven network modeling.

**Results:** Across modalities, trait-related abnormalities emerged. Relative to healthy comparison subjects, both clinical groups were characterized by lower rostral anterior cingulate cortex (rACC) GABA+ and frontoparietal network amplitude but higher amplitude in salience and stress-related networks. For

the remitted MDD group, differences from the healthy comparison group emerged in the context of elevated cortisol levels, whereas the MDD group had lower cortisol levels than the healthy comparison group. In the comparison group, frontoparietal and stress-related network connectivity was positively associated with cortisol level (highlighting putative top-down regulation of stress), but the opposite relationship emerged in the MDD and remitted MDD groups. Finally, rACC GABA+ was associated with stress-induced changes in connectivity between overlapping default mode and salience networks.

**Conclusions:** Lifetime MDD was characterized by reduced rACC GABA+ as well as dysregulated cortisol-related interactions between top-down control (frontoparietal) and threat (task-related) networks. These findings warrant further investigation of the role of GABA in the vulnerability to and treatment of MDD.

*Am J Psychiatry* 2024; 181:639–650; doi: 10.1176/appi.ajp.20230382

Up to 80% of first major depressive episodes are preceded by major life stressors (1), highlighting the importance of understanding how stress impacts brain processes and circuits affected in major depressive disorder (MDD). Acute stress triggers bottom-up and top-down regulatory brain circuits (2). Specifically, perturbations to homeostasis activate the hypothalamic-pituitary-adrenal (HPA) axis and autonomic nervous system, resulting in the secretion of corticotropin and subsequently cortisol from the adrenal glands. In healthy

responses to stress, cortisol secretion is associated with limbic system deactivation (3) by means of top-down control processes subserved by the prefrontal cortex (4). This adaptive response is weakened in individuals with MDD, as manifested in reduced top-down control from frontal regions and exaggerated bottom-up threat signaling (5). Such interplay between cortical and limbic regions in stress circuitry calls for a network approach to investigations of acute stress. In this context, functional MRI (fMRI) combined with

See related features: **Editorial** by Dr. Akiki and Dr. Abdallah (p. 578) and **CME course** (online and p. 650)

independent component analysis—an unsupervised machine learning technique that identifies functional networks and network modeling to assess their interactions—appears particularly suited.

Menon's triple network model (6) identifies functional networks important for understanding process dysfunction in psychopathology (7). These include the frontoparietal control network (FPN), implicated in top-down cognitive control and regulation; the default mode network (DMN), critical for self-referential processes; and the salience network (SN), associated with the detection and evaluation of salient exteroceptive and interoceptive inputs. In healthy individuals, the FPN and SN increase activation during stimulus-driven cognitive and affective processing, and the DMN is associated with internally oriented thoughts and deactivates during tasks (8). In MDD, studies have shown increased DMN activation, associated with increased rumination (7), and decreased ability to deactivate the DMN during task conditions. Reduced FPN activation is also a key feature of MDD (9), with weakened top-down control over threat responses from limbic regions and maladaptive SN evaluation, resulting in ineffective engagement of the FPN and DMN (10). Further evidence highlights lower FPN-DMN connectivity and higher DMN-SN connectivity (10) in MDD, which may be associated with increased evaluation of self-referential thoughts.

Meta-analyses of responses to various task-based and physiological stressors in healthy individuals in fMRI and positron emission tomography studies implicate increases in activation in regions such as the prefrontal cortex, anterior cingulate cortex (ACC), midcingulate cortex, basal ganglia, insula, and amygdala and deactivation in the hippocampus (3, 11). Activation in many of these regions has been found to be negatively associated with steroid hormone responses in females (12); critically, these regions are all key nodes in the triple networks. Among healthy adults, increased SN amplitude (13) and decreased SN-DMN connectivity after stress have been described (14). Moreover, among cortisol responders, increases in amygdala connectivity with the DMN and medial prefrontal cortex (mPFC) were found (15). Under acute stress, decreases in amygdala connectivity with the dorsolateral prefrontal cortex (DLPFC) and ACC, key nodes of the FPN, have also been reported (16). Potentiated FPN-SN connectivity is thought to underlie stress recovery, through top-down control of internal threat evaluation (17). Collectively, these findings in healthy individuals suggest that stress (and associated cortisol release) decreases connectivity between limbic and prefrontal circuits, interrupting top-down control. However, cortisol response to stress is blunted in MDD (18), particularly in females (19), which may result in maladaptive responses in stress circuitry, although this relationship is unexplored. Critically, in individuals with current or remitted MDD (rMDD), acute stress induction was found to reduce activation in the ventromedial prefrontal cortex (vmPFC) (20). Moreover, in rMDD, stress-related activation and connectivity of the DLPFC, striatum, and amygdala emerged (20, 21). Collectively, these findings

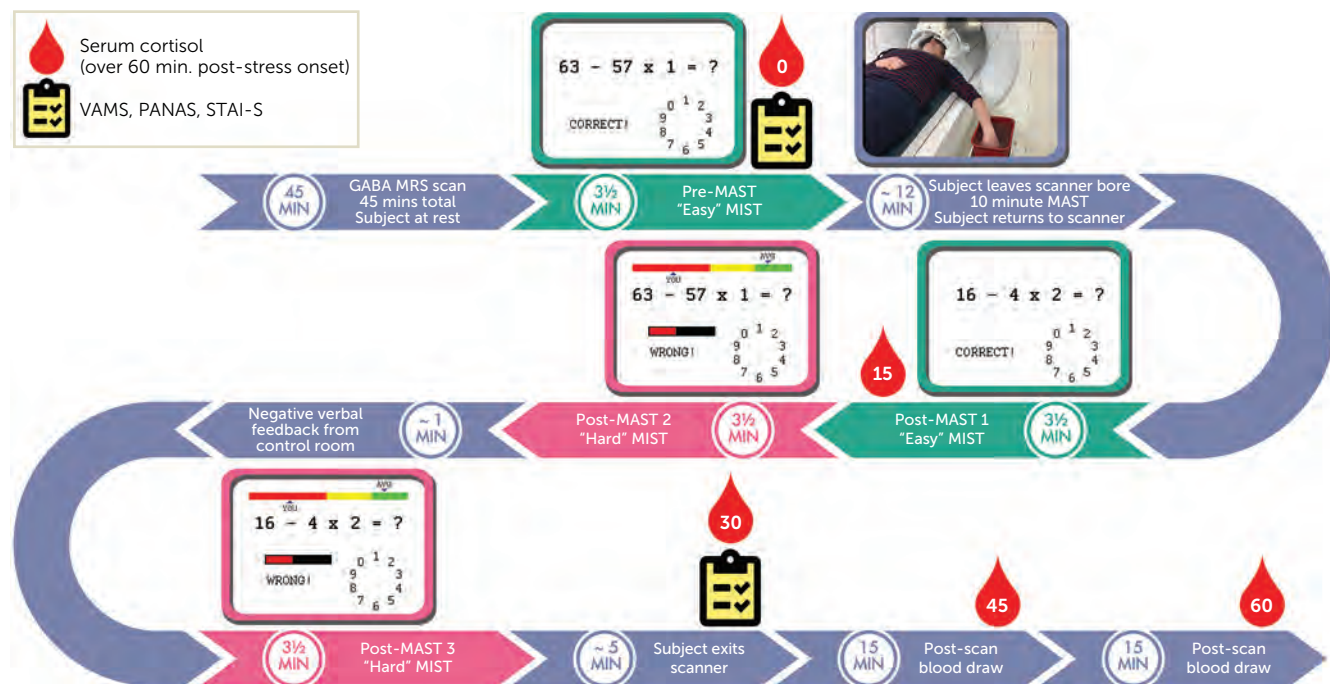
highlight interactions between limbic and cortical stress circuits that are impaired in a potentially trait-like fashion in MDD. Given reports of sex differences in this circuitry and the higher prevalence of MDD in females (22), an understanding of potential sex differences in cortisol and related neural responses to stress could contribute importantly to the overall understanding of MDD.

Multimodal neuroimaging research indicates that network activations and connectivity are affected by neuromodulators, especially inhibitory  $\gamma$ -aminobutyric acid (GABA) (23, 24). Reduced GABA levels have been observed in CSF (25) and cortical tissues (26) of patients with MDD, and in multiple brain regions using magnetic resonance spectroscopy (MRS) in patients with MDD and rMDD (27). Furthermore, recent findings suggest a negative relationship between DLPFC GABA+ ( $\gamma$ -aminobutyric acid and macromolecules) and resting-state functional connectivity between the DLPFC and mPFC in healthy comparison subjects not seen in MDD (24). We found in previous research that GABA+ was reduced in the rACC in females with MDD but not rMDD (28) and that GABA+ in this region was positively associated with connectivity between overlapping stress networks. These results point toward a potential mechanistic role for GABA in enabling top-down control that is impaired in MDD. However, relationships between GABA+ and network connectivity in the response to stress (and how this is affected by MDD and sex) are still poorly understood.

To address this gap, we combined multimodal neuroimaging with network modeling to assess the effects of acute stress in young adults with MDD and rMDD and matched healthy comparison subjects. Participants underwent multimodal imaging, with MRS GABA+ measurement in the rACC and left DLPFC at rest and fMRI during an acute stressor (Figure 1), with continuous blood cortisol measurements. We had four hypotheses:

1. Individuals with MDD (compared with healthy comparison subjects) would be characterized by reduced rACC and DLPFC GABA+ levels, blunted cortisol response, and aberrant stress-related changes in network amplitude and between-network connectivity in the FPN (decreased), SN (decreased), DMN (increased), and stress-related networks (increased). Given previous mixed findings (27, 28), it was unclear whether effects would be similar in MDD and rMDD; accordingly, an important goal was to clarify putative trait-versus-state effects.
2. There would be sex differences in GABA+ and stress reactivity, shown by relatively decreased GABA+ and cortisol response in females and differential engagement and connectivity of stress networks. This was expected to be driven by hyperactivity of limbic regions and hypoactivity of regulatory networks in females, particularly those with MDD.
3. Lower rACC and DLPFC GABA+ at rest would be associated with deficits in engaging and disengaging these networks under stress.

**FIGURE 1. Multimodal imaging at rest and with stressors in a study of stress response in young adults with lifetime depression<sup>a</sup>**



<sup>a</sup> Initial BOLD acquisition under baseline conditions (pre-MAST, untimed problems), followed by an acute stressor (MAST), followed by BOLD acquisition under stress conditions (post-MAST 1: untimed problems; post-MAST 2: timed problems and progress bar), followed by negative verbal feedback over the scanner intercom, followed by final BOLD acquisition (post-MAST 3: timed problems with progress bar). BOLD=blood-oxygen-level-dependent signal; GABA= $\gamma$ -aminobutyric acid; MAST=Maastricht Acute Stress Test; MIST=Montreal Imaging Stress Test; MRS=magnetic resonance spectroscopy; PANAS=Positive and Negative Affect Schedule; STAI-S=State-Trait Anxiety Inventory–State; VAMS=Visual Analogue Mood Scale. (Figure reprinted from reference 28 with permission from the publishers.)

4. GABA+ in regions overlapping with the networks of interest (rACC in SN and DLPFC in FPN) would moderate network amplitude and connectivity.

**METHODS**

**Participants**

A total of 130 unmedicated participants 18–25 years of age were recruited from the community. They provided written informed consent to a protocol approved by the Partners Human Research Committee. A clinician administered the Structured Clinical Interview for DSM-5. Forty-four participants (22 of them female) were assessed as currently having a major depressive episode (MDD group); 42 participants (22 of them female) had at least one prior major depressive episode, which was fully remitted (rMDD group); and 44 participants (21 of them female) were healthy comparison subjects. Participants were recruited by sex assigned at birth (65 females, 65 males), and all sex effects reported refer to sex assigned at birth. For the groups’ demographic information and clinical scores, see Tables S1 and S2 in the online supplement.

**Procedure**

The procedure has been described previously (28). Briefly, after insertion of an intravenous line, participants entered the MRI scanner. They completed a single ~45-minute

GABA MRS scan, followed by an acute laboratory stressor task during fMRI. To increase reliability of the imaging stressor, we combined the Montreal Imaging Stress Test (29) and the more potent Maastricht Acute Stress Test (MAST) (which has been shown to elicit robust autonomic, glucocorticoid, and affective stress responses [30]) into a single hybrid stressor (see Figure 1 and the online supplement).

**MRI and MRS Data Acquisition and Preprocessing**

A 3-T Siemens MAGNETOM Prisma scanner (Siemens Medical Systems, Iselin, N.J.) equipped with a 64-channel head coil was used to acquire high-resolution functional and structural MRI data. Functional MRI data were preprocessed using fMRIPrep, release 20.2.1 (31) (RRID: SCR\_016216), which is based on Nipype, release 1.5.1 (RRID: SCR\_002502).

For MRS acquisition, T<sub>1</sub>-weighted structural images were used to place voxels in the rACC (17.5 mL; 35×20×25 mm<sup>3</sup>) and left DLPFC (18.75 mL; 25×30×25 mm<sup>3</sup>) (32). GABA+ concentrations were normalized to water and corrected by percentage gray and white matter and CSF (see Figures S1 and S2 in the online supplement).

**Blood Cortisol Collection and Analysis**

We applied an established method for collecting HPA-axis hormone-level changes in response to acute stress using serial blood samples. Blood cortisol changes from stress were

calculated using area under the curve with respect to increase (AUCi) (see the online supplement).

### Independent Component Analysis of Functional Data

For a data-driven evaluation of network-level changes from stress, we ran a group independent component analysis of the fMRI data. The resulting independent component maps were thresholded using Gaussian-gamma mixture modeling with a significance threshold of  $p=0.5$  to identify the signals in each component. Five networks of interest were selected, and a dual regression approach (33) was used to extract network time courses for each participant by run. These were then used to estimate the amplitude of each network and connectivity between each network pair. Amplitude, a proxy for overall activation in each run, was defined as how much a network deviates from its own mean. Network connectivity between each network pair was defined as partial correlation in each run. Task-specific networks were extracted based on the runs and blocks of stress conditions (the task did not have trial-by-trial regressors).

### Network Modeling and Statistical Analysis

Network values were estimated by FSLNets, version 0.6 (34). Our main outcome variables (four repeated measures at one pre-stress and three post-stress time points) were 1) individual network amplitudes for each of the five networks and 2) between-network connectivity (network pairs). For single measurements of GABA+ and cortisol AUCi, outliers were first removed (determined by Cook's distance for the group-by-sex linear model), and linear regression was performed to evaluate group and sex differences and their interaction using the *lm* function in R (35). For repeated measures (main outcome network variables, self-report), mixed-effects regressions were conducted using the *lmerTest* package in R. Likelihood ratio tests were performed to determine whether sex and its interactions with other variables should be included in each model, and sex was retained in the model for only one network (DMN amplitude). To evaluate both clinical groups separately, we defined a priori contrasts as 1) the healthy comparison group versus the MDD group and 2) the healthy comparison group versus the rMDD group. Models were evaluated for main effects and interactions using analysis of variance, and fixed effects of contrasts were examined to establish the stress time point (post-MAST 1, post-MAST 2, post-MAST 3) or group (MDD, rMDD) driving significant effects. Follow-up tests using estimated marginal means were applied to evaluate trait-versus-state effects by comparing the MDD and rMDD groups. Effect sizes were calculated using the *r2glmm* package in R.

To leverage multimodal data, we regressed connectivity and amplitude values on stress, group, and sex as above and added rACC GABA+, DLPFC GABA+, or cortisol AUCi. All potential interaction terms were included, and network analyses were corrected for multiple comparisons using the false discovery rate for 145 tests (15 network amplitude and

connectivity pair models [main effects and interactions, three to seven tests per network model, depending on inclusion of sex in the model], as well as with cortisol [two additional interactions of interest per network model] and two GABA regions of interest [two additional interactions per network model per region of interest]; see Table S4 in the online supplement for a full list of the models and tests). False discovery rate-corrected  $p$  values are reported. Finally, to explore the relationship between self-report and biological markers of stress response, we correlated GABA+, cortisol AUCi, and significant network changes from stress with changes in affective ratings.

## RESULTS

### Group Independent Components Analysis

Five networks were selected a priori and identified from the group independent component analysis results (Figure 2): three networks corresponding to those highlighted in the triple network model (DMN, FPN, SN) (6) and two stressor task-specific networks (i.e., utilizing the task-specific nature of the independent component analysis data). For the task-specific networks, the first encompassed the temporal lobe, anterior insula, and amygdala (Temp-Ins-Amyg), and the second included the vmPFC, ventral striatum, and ACC (vmPFC-Str-ACC).

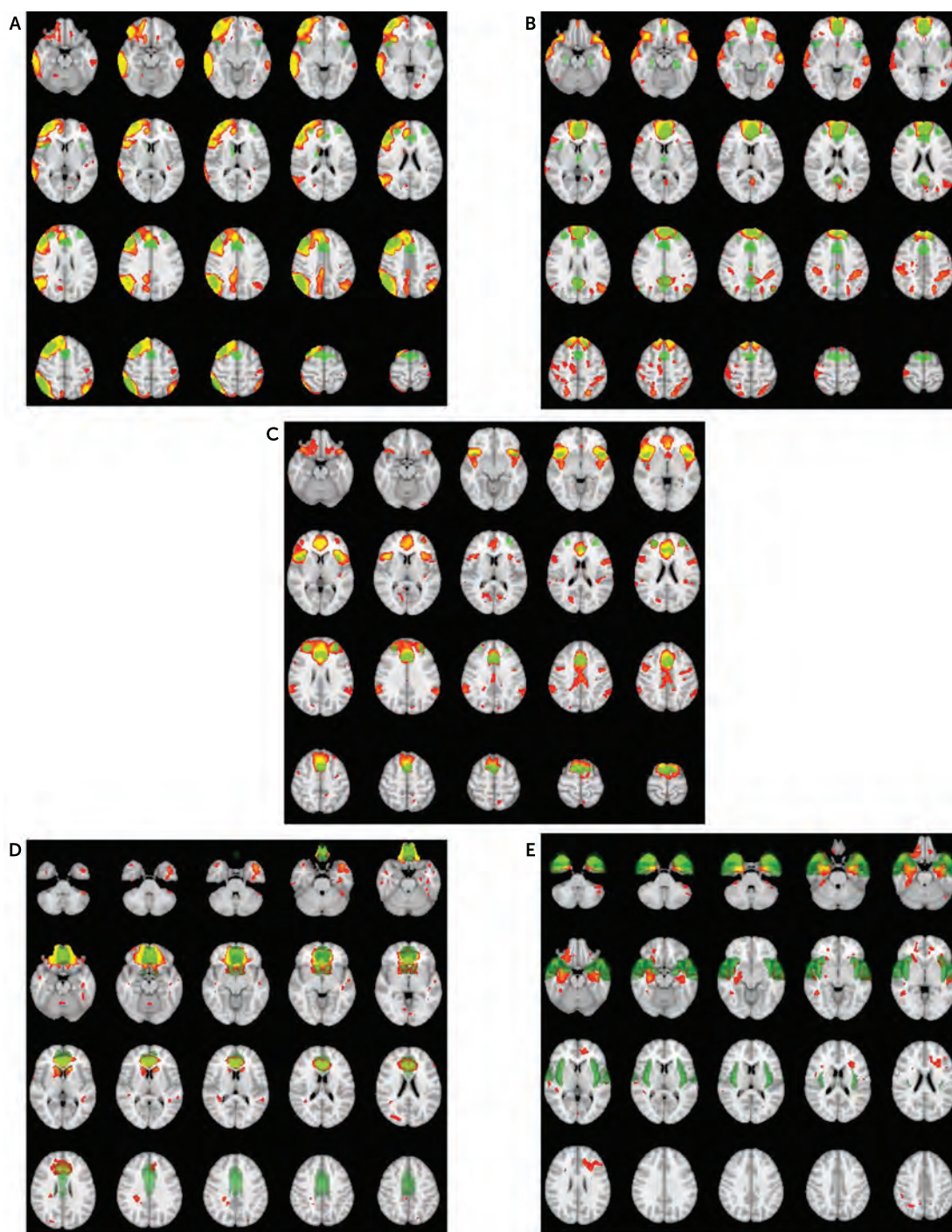
### Stress Results

A one-sample  $t$  test on the cortisol AUCi revealed that cortisol concentrations were significantly increased across participants ( $t=7.37$ ,  $df=88$ ,  $p<0.001$ ), indicating that the stressor elicited the intended effect. AUCi was then regressed on between-subject factors of group (healthy, MDD, rMDD) and sex (female, male) and their interaction. The interaction was not significant, but, in line with hypotheses 1 and 2, there were significant main effects of group ( $F=9.88$ ,  $df=2$ ,  $83$ ,  $p<0.001$ ) and sex, with males having significantly higher AUCi than females ( $\beta=0.51$ ,  $F=7.29$ ,  $df=1$ ,  $83$ ,  $p=0.008$ ,  $R^2=0.08$ ). Fixed effects clarified that the MDD group had significantly lower cortisol AUCi than the healthy comparison group ( $\beta=-0.40$ ,  $t=-2.98$ ,  $df=83$ ,  $p=0.004$ ,  $R^2=0.10$ ), whereas the rMDD group had significantly higher cortisol AUCi than the healthy comparison group ( $\beta=0.60$ ,  $t=4.397$ ,  $df=83$ ,  $p<0.001$ ,  $R^2=0.19$ ) (Figure 3). There was also a main effect of stress on all affective rating measures (all  $p$  values  $<0.001$ ), indicating that the stressor increased negative affect and decreased positive affect (see Figure S3 in the online supplement).

### GABA MRS Results

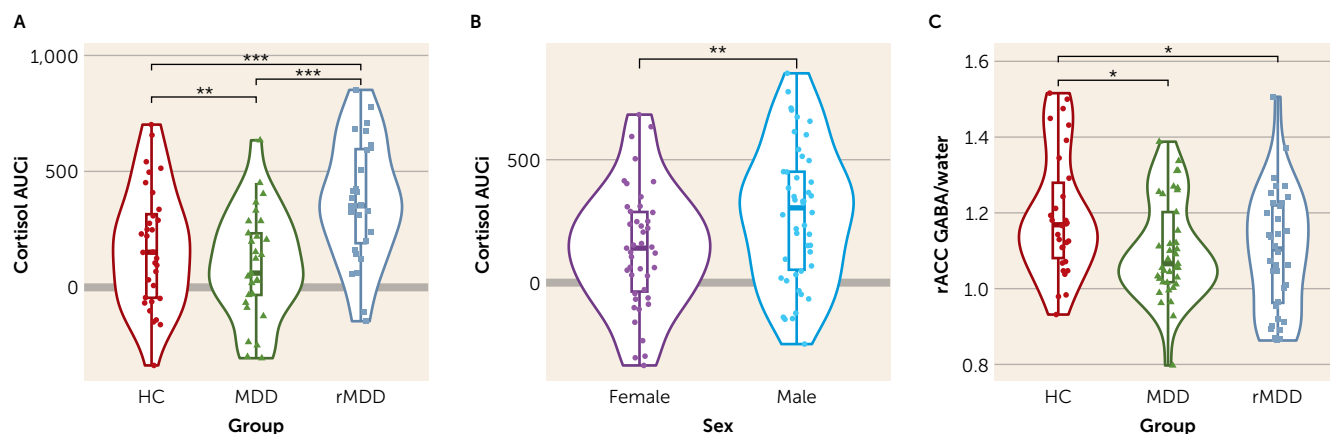
GABA+ values from the rACC and DLPFC were regressed on between-subject factors of group, sex, and their interaction. The interactions were not significant, but for the rACC only, a main effect of group emerged ( $F=4.01$ ,  $df=2$ ,  $97$ ,  $p_{corr}=0.04$ ). Follow-up tests showed that (as per hypothesis 1) the MDD and rMDD groups had significantly lower levels of

**FIGURE 2. Thresholded statistical maps of networks identified with group independent component analysis overlaid with canonical network maps and regions of interest<sup>a</sup>**



<sup>a</sup> Panel A shows the right frontoparietal network (3.39% of the variance explained) (red/yellow) overlaid with "right dorsolateral prefrontal cortex/right parietal" (green) from the Shirer et al. atlas (43). Panel B shows the default mode network (3.69% of the variance explained) (red/yellow) overlaid with "posterior cingulate cortex/ventromedial prefrontal cortex" (green) from the Shirer et al. atlas. Panel C shows the salience network (2.73% of the variance explained) (red/yellow) overlaid with "insula/dorsal anterior cingulate cortex" (green) from the Shirer et al. atlas. Panel D shows the ventromedial prefrontal cortex, ventral striatum, and anterior cingulate cortex (2.36% of the variance explained) (red/yellow) overlaid with unthresholded Harvard-Oxford cortical and subcortical atlas masks for the medial frontal cortex; cingulate gyrus, anterior division; right accumbens; and left accumbens (green). Panel E shows the temporal-insula-amygdala network (2.25% of the variance explained) (red/yellow) overlaid with unthresholded Harvard-Oxford cortical and subcortical atlas masks for the insular cortex; temporal pole; superior temporal gyrus, anterior division; inferior temporal gyrus, anterior division; left amygdala; and right amygdala (green). The percentage of variance explained is the amount of independent variance a component explains over and above all other components, divided by the sum of all unique amounts.

**FIGURE 3. Violin plots showing differences in cortisol response to stress, by group and by sex, and rostral anterior cingulate cortex GABA+ level, by group<sup>a</sup>**



<sup>a</sup> Cortisol response is measured by area under the curve with respect to increase (AUCi). Overlaid box plots show the median and interquartile range. GABA=γ-aminobutyric acid; HC=healthy comparison group; MDD=current major depressive disorder group; rACC=rostral anterior cingulate cortex; rMDD=remitted major depressive disorder group. \*p<0.05. \*\*p<0.01. \*\*\*p<0.001.

rACC GABA+ than the healthy comparison group (MDD:  $\beta = -0.09$ ,  $t = -2.49$ ,  $df = 97$ ,  $p = 0.01$ ,  $R^2 = 0.03$ ; rMDD:  $\beta = -0.1$ ,  $t = -2.58$ ,  $df = 97$ ,  $p = 0.01$ ,  $R^2 = 0.02$ ) (Figure 3C) but did not differ significantly from each other ( $\beta = -0.005$ ,  $t = -0.13$ ,  $df = 97$ ,  $p = 0.89$ ).

**fMRI Results: Effects of Stress**

Compared with pre-stress measures, stress significantly decreased amplitude in the FPN ( $F = 7.43$ ,  $df = 3$ ,  $348$ ,  $p_{corr} = 0.002$ ; post-MAST 2:  $\beta = -0.28$ ,  $R^2 = 0.01$ ; post-MAST 3:  $\beta = -0.26$ ,  $R^2 = 0.01$ ) and the DMN ( $F = 7.21$ ,  $df = 3$ ,  $342$ ,  $p_{corr} = 0.002$ ,  $R^2 = 0.02$ ; post-MAST 2:  $\beta = -0.30$ ,  $R^2 = 0.01$ ; post-MAST 3:  $\beta = -0.34$ ,  $R^2 = 0.02$ ), and increased amplitude in the two stress-related networks (Temp-Ins-Amyg:  $F = 13.82$ ,  $df = 3$ ,  $348$ ,  $p_{corr} < 0.001$ ; post-MAST 2:  $\beta = 0.54$ ,  $R^2 = 0.04$ ; post-MAST 3:  $\beta = 0.35$ ,  $R^2 = 0.02$ ; vmPFC-Str-ACC:  $F = 9.20$ ,  $df = 3$ ,  $348$ ,  $p_{corr} < 0.001$ ; post-MAST 2:  $\beta = 0.42$ ,  $R^2 = 0.02$ ; post-MAST 3:  $\beta = 0.24$ ,  $R^2 = 0.01$ ). Stress decreased connectivity between the DMN and SN ( $F = 8.89$ ,  $df = 3$ ,  $353$ ,  $p_{corr} < 0.001$ ; post-MAST 2:  $\beta = -0.45$ ,  $R^2 = 0.03$ ; post-MAST 3:  $\beta = 0.52$ ,  $R^2 = 0.03$ ) and increased connectivity between the DMN and FPN ( $F = 24.74$ ,  $df = 3$ ,  $352$ ,  $p_{corr} < 0.001$ ; post-MAST 2:  $\beta = 0.59$ ,  $R^2 = 0.02$ ; post-MAST 3:  $\beta = 0.46$ ,  $R^2 = 0.01$ ).

**fMRI Results: Effects of Diagnosis and Sex**

There was a main effect of group on FPN amplitude across the task ( $F = 8.64$ ,  $df = 2$ ,  $119$ ,  $p_{corr} = 0.005$ ) (Figure 4A). As per hypothesis 1, this was driven by the healthy comparison group having higher activation than the MDD and rMDD groups. Examination of the fixed effects showed that this main effect of group was driven by the MDD<healthy contrast ( $\beta = -0.29$ ,  $t = -2.42$ ,  $df = 278$ ,  $p = 0.02$ ,  $R^2 = 0.01$ ). Follow-up least square mean tests showed that rMDD<healthy ( $\beta = -0.23$ ,  $t = -3.76$ ,  $df = 121$ ,  $p < 0.001$ ,  $R^2 = 0.005$ ) and MDD=rMDD

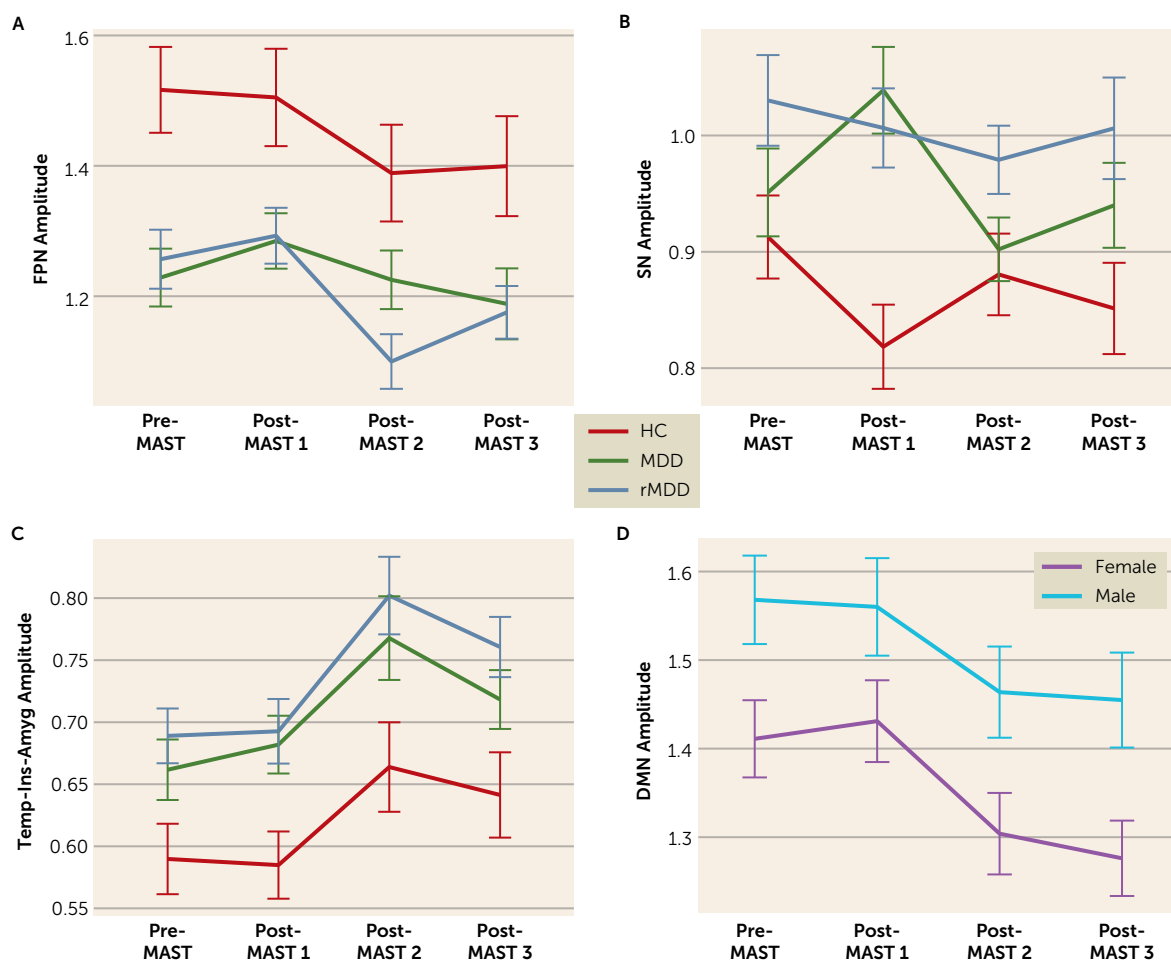
( $\beta = -0.02$ ,  $t = -0.34$ ,  $df = 120$ ,  $p = 0.73$ ). In contrast, we observed the opposite pattern in the SN and the Temp-Ins-Amyg network, with a main effect of group on amplitude across the task (SN:  $F = 7.99$ ,  $df = 2$ ,  $119$ ,  $p_{corr} = 0.007$ ; Temp-Ins-Amyg:  $F = 7.77$ ,  $df = 2$ ,  $117$ ,  $p_{corr} = 0.008$ ) (Figure 4B,C), driven by the healthy comparison group having lower amplitude than the MDD and rMDD groups. This main effect of group was driven by the rMDD>healthy contrast in the SN ( $\beta = 0.28$ ,  $t = 2.19$ ,  $df = 368$ ,  $p = 0.03$ ,  $R^2 = 0.01$ ). Follow-up least square mean tests showed that in both networks, MDD and rMDD>healthy (pairwise comparisons, all p values <0.01) and MDD=rMDD (pairwise comparisons, all p values >0.17).

In partial support of hypothesis 2, a main effect of sex emerged for DMN amplitude ( $F = 9.80$ ,  $df = 1$ ,  $118$ ,  $p_{corr} = 0.03$ ) (Figure 4D), driven by females having lower amplitude than males ( $\beta = -0.42$ ,  $t = -2.41$ ,  $df = 325$ ,  $p = 0.02$ ,  $R^2 = 0.01$ ).

**Associations of Network Changes From Stress With GABA+ and Cortisol**

Across all participants, there was a significant effect of DLPFC GABA+ on FPN amplitude change from stress (stress-by-DLPFC GABA+:  $F = 4.39$ ,  $df = 3$ ,  $288$ ,  $p_{corr} = 0.05$ ) (Figure 5A), with increased DLPFC GABA+ associated with greater reductions in FPN amplitude from stress (Pearson  $r = -0.28$ ,  $df = 87$ ,  $p = 0.006$ ). In addition, stress-induced DMN-SN connectivity changes were differentially associated with rACC GABA+ by clinical group (group-by-stress-by-rACC GABA+:  $F = 4.26$ ,  $df = 6$ ,  $275$ ,  $p_{corr} = 0.005$ ) (Figure 5B). This interaction was due to the fact that for the healthy comparison group—but not the clinical groups—higher GABA+ levels in the rACC were associated with lower DMN-SN connectivity ( $r = -0.40$ ,  $df = 25$ ,  $p = 0.04$ ). Critically, the rACC voxel overlaps these network pairs (see Figure S4 in the online supplement).

**FIGURE 4. Group differences in network amplitude in frontoparietal network, salience network, and temporal-insula-amygdala network and sex differences in default mode network<sup>a</sup>**



<sup>a</sup> Error bars indicate standard error of the mean. DMN=default mode network; FPN=frontoparietal network; HC=healthy comparison group; MAST=Maastricht Acute Stress Test; MDD=current major depressive disorder group; rMDD=remitted major depressive disorder group; SN=salience network; Temp-Ins-Amyg=temporal, insula, amygdala network.

Stress-induced FPN–Temp-Ins-Amyg connectivity changes were differentially associated with cortisol by group (group-by-stress-by-cortisol AUCi:  $F=3.61$ ,  $df=6$ ,  $240$ ,  $p_{corr}=0.03$ ) (Figure 5C); specifically, for the healthy comparison group, higher cortisol responses were associated with greater connectivity between the FPN and the Temp-Ins-Amyg network ( $r=0.41$ ,  $df=30$ ,  $p=0.02$ ). For both the MDD ( $r=-0.45$ ,  $df=24$ ,  $p=0.02$ ) and rMDD ( $r=-0.38$ ,  $df=26$ ,  $p=0.05$ ) groups, a negative association emerged.

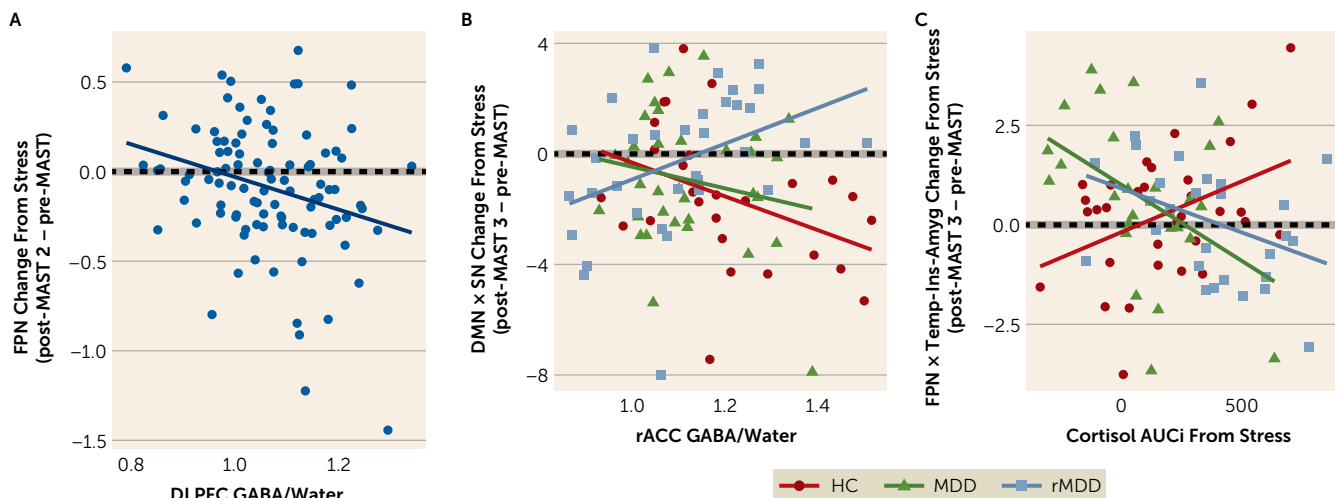
Table 1 summarizes the directionality of significant findings. To aid interpretation of relationships between our multiple measures, exploratory correlational analyses were run (see Figure S5 in the online supplement).

## DISCUSSION

Acute stress affected four networks of interest: The FPN and DMN decreased amplitude under acute stress, whereas stress-related networks (vmPFC-Str-ACC and Temp-Ins-Amyg) predictably increased amplitude. Per hypothesis 1,

young adults with MDD had lower cortisol AUCi than healthy comparison subjects, whereas, unexpectedly, those in remission (rMDD) had higher cortisol than healthy subjects. Moreover, compared with healthy subjects, those with MDD or rMDD showed lower rACC GABA+, lower FPN amplitude, and higher SN and Temp-Ins-Amyg amplitude, partially supporting hypothesis 1 and suggesting a trait-like effect of MDD on GABA+ and these networks. Critically, cortisol response to stress in the healthy comparison group was positively associated with stress-related changes in “top-down, bottom-up” connectivity between a network associated with top-down control (FPN) and a bottom-up threat-related task network (Temp-Ins-Amyg), whereas the opposite was the case for the MDD and rMDD groups, where cortisol was associated with reduced top-down, bottom-up connectivity. Dimensionally, this change in top-down, bottom-up connectivity was positively associated with hostility emerging throughout the stress manipulation (see the online supplement) and negatively associated with changes in connectivity between the

**FIGURE 5. Associations of cortisol and GABA+ with network amplitude and connectivity changes from stress<sup>a</sup>**



<sup>a</sup> Panel A shows the association of DLPFC GABA+ with frontoparietal amplitude changes from stress. Panel B shows the association of rACC GABA+ with default mode network-by-salience network connectivity changes from stress. Panel C shows the associations of cortisol response from stress with changes from stress in frontoparietal network-by-temporal-insula-amygdala network connectivity. AUCi=area under the curve with respect to increase; DLPFC=dorsolateral prefrontal cortex; DMN=default mode network; FPN=frontoparietal network; GABA= $\gamma$ -aminobutyric acid; HC=healthy comparison group; MAST=Maastricht Acute Stress Test; MDD=current major depressive disorder group; rACC=rostral anterior cingulate cortex; rMDD=remitted major depressive disorder group; SN=salience network; Temp-Ins-Amyg=temporal, insula, amygdala network.

evaluative SN and self-referential DMN. Partially supporting hypotheses 3 and 4, increased rACC GABA+ was also associated with stress-related reductions in putatively evaluative and self-referential connectivity (SN-DMN connectivity) in healthy subjects, whereas this was not the case in those with MDD and rMDD. Across participants, there was also a negative relationship between this SN-DMN and SN-Temp-Ins-Amyg connectivity, suggesting that external (threat-related) evaluation might increase when internal self-referential evaluation decreases. In terms of sex differences, in partial support of hypothesis 2, males showed higher cortisol response than females overall, and males were characterized by hyperactive DMN compared with females. See Figure 6 for a graphical representation and integration of the findings.

Healthy stress responses involve cortisol release, effective salience evaluation (SN), and top-down control over bottom-up limbic regions that signal threat (Temp-Ins-Amyg) by increasing connectivity with the FPN (36). These networks have also emerged in meta-analyses of stress circuitry in healthy subjects (11). Our findings suggest that those with MDD or rMDD had lower FPN activation, pointing to impaired top-down signaling. Conversely, the clinical groups had higher activation in the evaluative SN and the stress-related network (Temp-Ins-Amyg), suggesting exaggerated bottom-up threat signaling. Similar to previous findings (19), we observed a blunted cortisol response to stress in individuals with MDD and lower cortisol response in females compared with males. The reduced cortisol response in MDD seems to be state-dependent, and higher cortisol response in rMDD may be an important biological marker of remission, potentially representing a reengagement of emotional responding, which can be blunted in MDD (37). Hypoactivation of the stress response circuitry in

females with MDD has previously been shown to relate to dysregulation of hypothalamic-pituitary-gonadal-axis hormones, which may be an important mechanism underlying sex differences in MDD prevalence (22).

Together, these findings suggest a key role for rACC GABA+ in downstream network amplitude and both rACC GABA+ and cortisol in downstream cortico-limbic between-network connectivity under stress, elucidating potential network effects of previously shown deleterious effects of stress on prefrontal GABA (38). Rostral ACC GABA+ was lower in those with MDD and rMDD who also showed lower top-down (FPN) and higher evaluative (SN) and threat signaling (Temp-Ins-Amyg) activation. We speculate that these patterns collectively highlight blunted stress response in current MDD, which may lead to increased evaluative SN and bottom-up threat-related activation, thereby increasing reliance on automatic responses and lowering demand on the FPN to exert top-down control. This was further supported by dimensional analyses showing that rACC GABA+ was associated with stress-induced decreases in connectivity between the evaluative SN and self-referential DMN in the healthy comparison group but not in the clinical groups, who may lack effective inhibition of these networks under stress. This extends previous findings on healthy inhibitory relationships between GABA+ and DMN and top-down control network connectivity (24) being imbalanced in psychopathology (23). We also observed negative exploratory correlations between this evaluative and self-referential network and networks associated with top-down, bottom-up engagement, suggesting that these processes move in opposite directions following stress.

GABA MRS data add a new dimension to the role of rACC inhibition in stress, with higher rACC GABA+ being

associated with a stress-related decrease in evaluative and self-referential connectivity between the SN (which overlaps the MRS voxel) and the DMN. Lower GABAergic inhibition in the rACC in MDD and rMDD could result in exaggerated or maladaptive self-referential evaluation, whereas the healthy response to stress would be to inhibit this network in favor of engaging top-down control (FPN) and evaluation (SN) of threat signals (Temp-Ins-Amyg). Our exploratory correlations shed further light on this relationship, with rACC GABA+ associated decreases in proposed maladaptive evaluative and self-referential connectivity being linked to increases in more adaptive top-down, bottom-up connectivity and threat evaluation connectivity. A recent trial of positive allosteric modulator of GABA<sub>A</sub> receptors has shown promising results in the treatment of MDD (39). An interesting next step might be to test whether GABAergic treatments reduce stress-induced maladaptive self-referential evaluation or increase top-down control and evaluation of threat signals.

The findings suggest potentially interesting overall sex differences, with lower DMN amplitude in females compared with males. Diminished deactivation of the DMN during a task has been reported previously in rMDD (40), but previous studies have not examined sex differences. Our finding that females deactivated the DMN during a stressor task to a greater extent than males suggests a potential difference in a network previously implicated in treatment. This could be explained by males showing later development than females of prefrontal circuits that regulate the DMN (41). This may mean that treatments to reduce self-referential processing and DMN activation may be more effective in young females than young males.

Our hypothesis that MDD would be characterized by reduced DLPFC GABA+ levels was not supported, and, as most group effects were main effects (or interactions with cortisol and GABA), we show limited evidence of aberrant stress-related changes in network amplitude and between-network connectivity. We also did not show sex differences in GABA+ or differential between-network connectivity of stress networks.

Limitations of the study include the lack of group differences in network response to stress when not considering cortisol or GABA, few group-by-sex differences (although this may reflect a lack of statistical power, as indicated by larger minimum effect sizes in supplemental sensitivity analyses of power), the use of data-driven techniques to test specific hypotheses, and the lack of a behavioral measure in our task. However, our repeated-measures design and inclusion of unmedicated young adults under age 26 (selected a priori to account for PFC maturation), as well as control for menstrual cycle and time of day, improved the rigor and statistical power. We did not find differences in DLPFC GABA+, despite recent evidence (27). Also, among a subset of the healthy comparison subjects, we previously reported that the test-retest reliability of the rACC voxel was low to moderate (32). We analyzed effects of sex assigned at birth, and the parent study will examine gonadal hormones.

**TABLE 1. Directionality of significant GABA, cortisol, and imaging findings in a study of stress response in young adults with lifetime depression<sup>a</sup>**

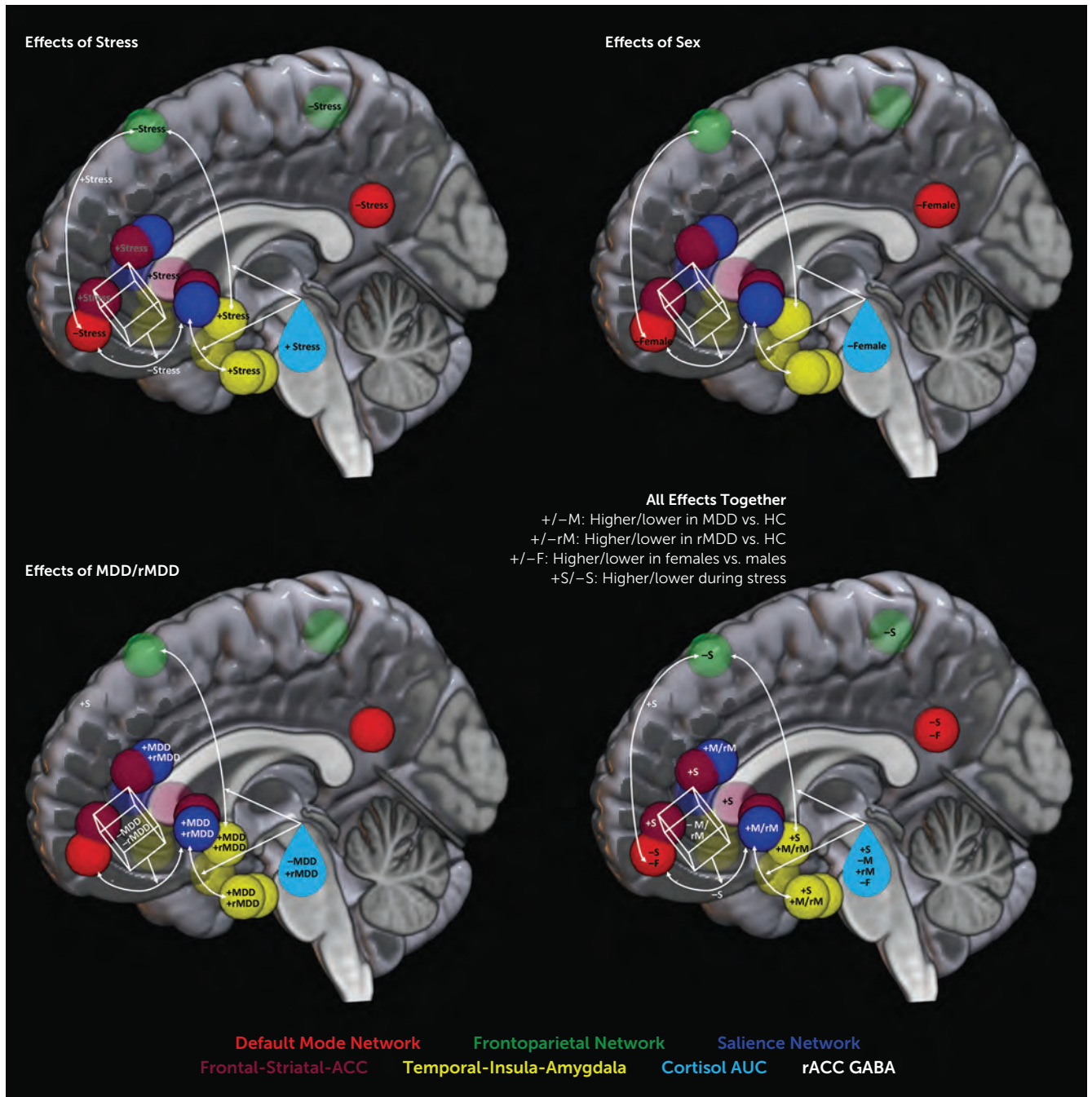
Measure	Overall Effect	Effect of Stress
rACC GABA	MDD<HC rMDD<HC	
Cortisol AUCi		Increased from stress MDD<HC rMDD<HC Female<male
FPN amplitude	MDD<HC rMDD<HC	Decreased from stress DLPFC GABA correlated with decrease
DMN amplitude SN amplitude	Female<male HC<MDD HC<rMDD	Decreased from stress
Temp-Ins-Amyg amplitude	HC<MDD HC<rMDD	Increased from stress
vmPFC-Str-ACC amplitude		Increased from stress
DMN-SN connectivity		Decreased from stress Group-by-rACC GABA
DMN-FPN connectivity FPN-Temp-Ins-Amyg connectivity		Increased from stress Group-by-cortisol AUCi

<sup>a</sup> AUCi=area under the curve with respect to increase; DLPFC=dorsolateral prefrontal cortex; DMN=default mode network; FPN=right frontoparietal network; GABA=γ-aminobutyric acid; HC=healthy comparison group; MDD=current major depressive disorder group; rACC=rostral anterior cingulate cortex; rMDD=remitted major depressive disorder group; SN=salience network; Temp-Ins-Amyg=temporal, insula, amygdala network; vmPFC-Str-ACC=ventromedial prefrontal cortex, ventral striatum, anterior cingulate cortex network.

However, sex effects are often overlapping (42), and this study does not consider gender identity. Finally, the participants' young age, the lack of comorbidities, and the limited ecological validity of laboratory stressors limit generalizability.

In summary, the multimodal approach used in this study unveiled state- and trait-related abnormalities in MDD. We found that stress increased amplitude in networks associated with bottom-up threat signaling and coping and reduced amplitude in networks associated with top-down control and self-referential processing. In addition, compared with healthy subjects, young adults with MDD or rMDD had lower top-down control network amplitude and higher threat (bottom-up) and self-referential network amplitude, highlighting trait effects of MDD and rMDD. Importantly, cortisol response to stress showed a state effect, with blunting in the MDD group contrasting with potentiation in the rMDD group, and was associated with stress-induced increases in top-down, bottom-up connectivity in healthy subjects but not in the clinical groups. Sex differences in cortisol response to stress were associated with evaluative and bottom-up connectivity changes. Critically, lower rACC GABA+ was found to be a trait feature of MDD and rMDD and was associated with stress-induced connectivity changes in an evaluative and self-referential network critical to MDD pathophysiology. Together, these novel findings suggest that deficits in stress hormone signaling and

**FIGURE 6. Summary of model: brain surface rendering summarizing significant findings related to effects of stress, group, and sex<sup>a</sup>**



<sup>a</sup> ACC=anterior cingulate cortex; AUC=area under the curve; GABA=γ-aminobutyric acid; MDD=current major depressive disorder group; rACC=rostral anterior cingulate cortex; rMDD=remitted major depressive disorder group.

inhibitory GABAergic mechanisms have downstream effects on activation of, and connectivity between, networks implicated in stress and the pathophysiology of MDD.

**AUTHOR AND ARTICLE INFORMATION**

Center for Depression, Anxiety, and Stress Research (Ironsides, Duda, Moser, Perlo, Richards, Null, Esfand, Alexander, Crowley, Pizzagalli) and McLean Imaging Center (Zuo, Du, Chen, Nickerson, Pizzagalli), McLean

Hospital, Belmont, Mass.; Laureate Institute for Brain Research, Tulsa, Okla. (Ironsides); Harvard Medical School, Boston (Holsen, Zuo, Du, Chen, Nickerson, Misra, Goldstein, Pizzagalli); Division of Women’s Health, Department of Medicine (Holsen), and Department of Psychiatry, Brigham and Women’s Hospital, Boston (Holsen); Division of Pediatric Endocrinology (Lauze, Misra), Department of Psychiatry (Goldstein), and Innovation Center on Sex Differences in Medicine (Holsen, Misra, Goldstein), Massachusetts General Hospital, Boston.

Send correspondence to Dr. Pizzagalli (dap@mclean.harvard.edu).

Drs. Goldstein and Pizzagalli contributed equally as senior authors.

Supported by NIMH grant R01MH108602 (principal investigators, Drs. Pizzagalli and Goldstein).

Dr. Pizzagalli was supported in part by NIMH grant R37 MH068376. Drs. Goldstein and Holsen were partially supported by Office of Research on Women's Health–NIMH grant U54 MH118919 (principal investigators, Drs. Goldstein and Robert J. Handa). Dr. Ironside was supported in part by a Rappaport Mental Health Fellowship from McLean Hospital, center grant P20GM121312 from the National Institute of General Medical Sciences, and NIMH grant R01MH132565. Dr. Misra was supported in part by NIH grant R01DK124223 and NIMH grant R01MH116205.

The MEGA-PRESS sequence was developed by Edward J. Auerbach and Małgorzata Marjańska and provided by the University of Minnesota under a customer-to-partner agreement. This work was conducted with support from Harvard Catalyst–The Harvard Clinical and Translational Science Center (National Center for Advancing Translational Sciences award UL1 TR002541) and financial contributions from Harvard University and its affiliated academic health care centers.

The authors thank David Olson, M.D., for assistance with blood collection protocol and Courtney Miller for assistance with blood draws. The authors also thank Madeline (Lynn) Alexander, Ph.D., Laurie A. Scott, A.M., and Harlyn Aizley, Ed.M., for clinical interviews to establish study eligibility, Monica Landi, M.S.W., for her help in establishing diagnostic reliability, and Lewis Ironside for graphic design.

Dr. Misra has served on the advisory boards of AbbVie and Ipsen, served as a consultant for AbbVie and Sanofi, and served as a Key Opinion Leader for Lumos Pharmaceuticals; she has received study drug donations from Tonix Pharmaceuticals; and she is a contributor to UpToDate. Dr. Goldstein has served on the scientific advisory board of and has an equity interest in Cala Health. Dr. Pizzagalli has served as a consultant for Boehringer Ingelheim, Compass Pathways, Engrail Therapeutics, Neumora Therapeutics (formerly BlackThorn Therapeutics), Neurocrine Biosciences, Neuroscience Software, Otsuka, Sage Therapeutics, Sama Therapeutics, Sunovion Pharmaceuticals, and Takeda Pharmaceuticals; he has received honoraria from the American Psychological Association, the Psychonomic Society, and Springer (for editorial work) and from Alkermes; he has received research funding from the Bird Foundation, the Brain and Behavior Research Foundation, the Dana Foundation, Millennium Pharmaceuticals, and Wellcome Leap; and he has received stock options from Compass Pathways, Engrail Therapeutics, Neumora Therapeutics, and Neuroscience Software. The other authors report no financial relationships with commercial interests.

Received May 8, 2023; revisions received September 19 and December 7, 2023; accepted January 10, 2024; published online April 30, 2024.

## REFERENCES

- Hammen C: Stress and depression. *Annu Rev Clin Psychol* 2005; 1: 293–319
- Ulrich-Lai YM, Herman JP: Neural regulation of endocrine and autonomic stress responses. *Nat Rev Neurosci* 2009; 10:397–409
- Dedovic K, D'Aguiar C, Pruessner JC: What stress does to your brain: a review of neuroimaging studies. *Can J Psychiatry* 2009; 54: 6–15
- Friedman MJ: The human stress response, in *A Practical Guide to PTSD Treatment: Pharmacological and Psychotherapeutic Approaches*. Edited by Bernardy NC, Friedman MJ. Washington, DC, American Psychological Association, 2015, pp 9–19
- Siegle GJ, Thompson W, Carter CS, et al: Increased amygdala and decreased dorsolateral prefrontal BOLD responses in unipolar depression: related and independent features. *Biol Psychiatry* 2007; 61:198–209
- Menon V: Large-scale brain networks and psychopathology: a unifying triple network model. *Trends Cogn Sci* 2011; 15:483–506
- Kaiser RH, Andrews-Hanna JR, Wager TD, et al: Large-scale network dysfunction in major depressive disorder: a meta-analysis of resting-state functional connectivity. *JAMA Psychiatry* 2015; 72: 603–611
- Nickerson LD: Replication of resting state-task network correspondence and novel findings on brain network activation during task fMRI in the human connectome project study. *Sci Rep* 2018; 8: 17543
- Lui S, Wu Q, Qiu L, et al: Resting-state functional connectivity in treatment-resistant depression. *Am J Psychiatry* 2011; 168: 642–648
- Manoliu A, Meng C, Brandl F, et al: Insular dysfunction within the salience network is associated with severity of symptoms and aberrant inter-network connectivity in major depressive disorder. *Front Hum Neurosci* 2014; 7:930
- Qiu Y, Fan Z, Zhong M, et al: Brain activation elicited by acute stress: an ALE meta-analysis. *Neurosci Biobehav Rev* 2022; 132: 706–724
- Goldstein JM, Jerram M, Poldrack R, et al: Hormonal cycle modulates arousal circuitry in women using functional magnetic resonance imaging. *J Neurosci* 2005; 25:9309–9316
- van Marle HJ, Hermans EJ, Qin S, et al: Enhanced resting-state connectivity of amygdala in the immediate aftermath of acute psychological stress. *Neuroimage* 2010; 53:348–354
- Vaisvaser S, Lin T, Admon R, et al: Neural traces of stress: cortisol related sustained enhancement of amygdala-hippocampal functional connectivity. *Front Hum Neurosci* 2013; 7:313
- Dimitrov A, Demin K, Fehlner P, et al: Differences in neural recovery from acute stress between cortisol responders and non-responders. *Front Psychiatry* 2018; 9:631
- Quaedflieg CW, van de Ven V, Meyer T, et al: Temporal dynamics of stress-induced alternations of intrinsic amygdala connectivity and neuroendocrine levels. *PLoS One* 2015; 10:e0124141
- Hermans EJ, Henckens MJ, Joëls M, et al: Dynamic adaptation of large-scale brain networks in response to acute stressors. *Trends Neurosci* 2014; 37:304–314
- Peeters F, Nicholson NA, Berkhof J: Cortisol responses to daily events in major depressive disorder. *Psychosom Med* 2003; 65: 836–841
- Burke HM, Fernald LC, Gertler PJ, et al: Depressive symptoms are associated with blunted cortisol stress responses in very low-income women. *Psychosom Med* 2005; 67:211–216
- Ming Q, Zhong X, Zhang X, et al: State-independent and dependent neural responses to psychosocial stress in current and remitted depression. *Am J Psychiatry* 2017; 174:971–979
- Admon R, Holsen LM, Aizley H, et al: Striatal hypersensitivity during stress in remitted individuals with recurrent depression. *Biol Psychiatry* 2015; 78:67–76
- Holsen LM, Spaeth SB, Lee JH, et al: Stress response circuitry hypoactivation related to hormonal dysfunction in women with major depression. *J Affect Disord* 2011; 131:379–387
- Northoff G, Sibille E: Why are cortical GABA neurons relevant to internal focus in depression? A cross-level model linking cellular, biochemical and neural network findings. *Mol Psychiatry* 2014; 19: 966–977
- Chen X, Song X, Öngür D, et al: Association of default-mode network neurotransmitters and inter-network functional connectivity in first episode psychosis. *Neuropsychopharmacol* 2023; 48: 781–788
- Gerner RH, Hare TA: CSF GABA in normal subjects and patients with depression, schizophrenia, mania, and anorexia nervosa. *Am J Psychiatry* 1981; 138:1098–1101
- Gabbay V, Mao X, Klein RG, et al: Anterior cingulate cortex  $\gamma$ -aminobutyric acid in depressed adolescents: relationship to anhedonia. *Arch Gen Psychiatry* 2012; 69:139–149
- Ritter C, Buchmann A, Müller ST, et al: Evaluation of prefrontal  $\gamma$ -aminobutyric acid and glutamate levels in individuals with major depressive disorder using proton magnetic resonance spectroscopy. *JAMA Psychiatry* 2022; 79:1209–1216

28. Ironside M, Moser AD, Holsen LM, et al: Reductions in rostral anterior cingulate GABA are associated with stress circuitry in females with major depression: a multimodal imaging investigation. *Neuropsychopharmacology* 2021; 46:2188–2196

29. Dedovic K, Renwick R, Mahani NK, et al: The Montreal imaging stress task: using functional imaging to investigate the effects of perceiving and processing psychosocial stress in the human brain. *J Psychiatry Neurosci* 2005; 30:319–325

30. Smeets T, Cornelisse S, Quaedflieg CW, et al: Introducing the Maastricht Acute Stress Test (MAST): a quick and non-invasive approach to elicit robust autonomic and glucocorticoid stress responses. *Psychoneuroendocrinology* 2012; 37:1998–2008

31. Esteban O, Markiewicz CJ, Blair RW, et al: fMRIPrep: a robust preprocessing pipeline for functional MRI. *Nat Methods* 2019; 16: 111–116

32. Duda JM, Moser AD, Zuo CS, et al: Repeatability and reliability of GABA measurements with magnetic resonance spectroscopy in healthy young adults. *Magn Reson Med* 2021; 85:2359–2369

33. Nickerson LD, Smith SM, Öngür D, et al: Using dual regression to investigate network shape and amplitude in functional connectivity analyses. *Front Neurosci* 2017; 11:115

34. Smith SM, Vidaurre D, Beckmann CF, et al: Functional connectomics from resting-state fMRI. *Trends Cogn Sci* 2013; 17:666–682

35. R Development Core Team: R: a Language and Environment for Statistical Computing. Vienna, Va, R Foundation for Statistical Computing, 2013

36. Pruessner JC, Dedovic K, Khalili-Mahani N, et al: Deactivation of the limbic system during acute psychosocial stress: evidence from positron emission tomography and functional magnetic resonance imaging studies. *Biol Psychiatry* 2008; 63:234–240

37. Burke HM, Davis MC, Otte C, et al: Depression and cortisol responses to psychological stress: a meta-analysis. *Psychoneuroendocrinology* 2005; 30:846–856

38. Hasler G, van der Veen JW, Grillon C, et al: Effect of acute psychological stress on prefrontal GABA concentration determined by proton magnetic resonance spectroscopy. *Am J Psychiatry* 2010; 167:1226–1231

39. Gunduz-Bruce H, Silber C, Kaul I, et al: Trial of SAGE-217 in patients with major depressive disorder. *N Engl J Med* 2019; 381: 903–911

40. Bartova L, Meyer BM, Diers K, et al: Reduced default mode network suppression during a working memory task in remitted major depression. *J Psychiatr Res* 2015; 64:9–18

41. Gennatas ED, Avants BB, Wolf DH, et al: Age-related effects and sex differences in gray matter density, volume, mass, and cortical thickness from childhood to young adulthood. *J Neurosci* 2017; 37: 5065–5073

42. Maney DL: Perils and pitfalls of reporting sex differences. *Philos Trans R Soc Lond B Biol Sci* 2016; 371:20150119

43. Shirer WR, Ryali S, Rykhlevskaia E, et al: Decoding subject-driven cognitive states with whole-brain connectivity patterns. *Cereb Cortex* 2012; 22:158–165

**Continuing Medical Education**

You can earn CME credits by reading this article. Three articles in every *American Journal of Psychiatry* issue comprise a short course for up to 1 *AMA PRA Category 1 Credit™* each. The course consists of reading the article and answering three multiple-choice questions with a single correct answer. CME credit is issued only online. Readers who want credit must subscribe to the AJP Continuing Medical Education Course Program ([psychiatryonline.org/cme](http://psychiatryonline.org/cme)), select *The American Journal of Psychiatry* at that site, take the course(s) of their choosing, complete an evaluation form, and submit their answers for CME credit. A certificate for each course will be generated upon successful completion. This activity is sponsored by the American Psychiatric Association.

**Examination Questions for “Association of Lower Rostral Anterior Cingulate GABA+ and Dysregulated Cortisol Stress Response With Altered Functional Connectivity in Young Adults With Lifetime Depression: A Multimodal Imaging Investigation of Trait and State Effects”**

1. Which of the following combinations of canonical resting-state networks showed decreased amplitude following an acute laboratory stressor?
  - A. Frontoparietal network, default mode network
  - B. Frontoparietal network, salience network
  - C. Default mode network, salience network
  - D. Frontoparietal network, default mode network, salience network
2. What was the directionality of the significant differences in rostral anterior cingulate cortex GABA+ between the three groups (healthy comparisons [HC], major depressive disorder [MDD], and remitted major depressive disorder [rMDD])?
  - A. MDD < rMDD < HC
  - B. MDD < HC < rMDD
  - C. MDD = rMDD < HC
  - D. HC < rMDD < MDD
3. Stress induced connectivity changes between which two networks was negatively associated with rostral anterior cingulate cortex GABA+ for healthy comparisons but not either of the clinical groups?
  - A. Frontoparietal network, default mode network
  - B. Default mode network, salience network
  - C. Default mode network, task network (temporal-insula-amygdala)
  - D. Frontoparietal network, salience network

Data supplement for Ironside et al., Association of Lower Rostral Anterior Cingulate GABA+ and Dysregulated Cortisol Stress Response With altered Functional Connectivity in Young Adults With Lifetime depression: A Multimodal Imaging Investigation of Trait and State Effects. *Am J Psychiatry* (doi: 10.1176/appi.ajp.20230382)

## **Supplemental Methods**

### *Participants*

Inter-rater reliability was assessed using audiotapes of subject interviews that were independently, blindly rated by a second interviewer. Two McLean-based study interviewers rated audiotapes consisting of the Structured Clinical Interview for DSM-5 Disorders (SCID-5 (1)), Hamilton Depression Rating Scale (HDRS (2)), and Quick Inventory of Depressive Symptomatology (QIDS (3)) interviews conducted by one of the other three study interviewers, including one based at the Brigham and Women's Hospital site. The 28 tapes (15% of the sample) that were included were randomly selected from within each of three diagnostic categories (MDD, remitted MDD, and not meeting criteria for either current or past depression) by a staff member not involved in the inter-rater reliability process. An intraclass correlation of 0.95 was obtained for the 17-item total HDRS score, and an intraclass correlation coefficient of 0.96 was obtained for the 16-item total QIDS score. Assessment of the diagnostic agreement of MDD vs. rMDD vs. no history of MDD yielded a kappa coefficient of 0.94.

For gender identity, two participants identified as non-binary, 64 as cisgender women, and 64 as cisgender men. Age of onset of first MDE did not differ significantly between the MDD ( $M = 16.8$ ,  $SD = 3.5$ ) and rMDD ( $M = 17.6$ ,  $SD = 2.4$ ) groups ( $t(76) = 1.19$ ,  $p = 0.2$ ) but number of depressive episodes did, with the MDD group reporting a median of 2 and the rMDD group reporting a median of 1 (Wilcoxon test:  $W = 1230$ ,  $p = 0.004$ ). Exclusion criteria included other comorbid psychiatric disorders, use of

psychoactive drugs, recent recreational drug use or past substance use disorder. Recent recreational drug use was ruled out with a urine drug test carried out at screening and testing days. Participants were compensated for their time. Participants needed a washout period for psychoactive drugs of six weeks for fluoxetine, two weeks for any other antidepressants or benzodiazepines. Demographics are summarized in Table S1.

### ***Procedure***

The imaging session took place in the early follicular phase (first seven days, although there were three participants, one in each group, who we allowed up to day 11 because of longer cycles) of the female participants' menstrual cycle to control for hormonal variability and in the afternoon, to control for diurnal variability of cortisol response (4). To improve the potency of the stressor following piloting, the protocol combined the MIST (5) and the Maastricht Acute Stress Test (6) into a single hybrid stressor. As depicted in main text Figure 1, participants completed four blocks of arithmetic problems, each lasting ~3.5 min. During block one (pre-MAST), there was no time pressure and participants received trial-by-trial performance feedback ("correct", "incorrect"). This constituted a "no-stress" baseline condition. After the first block, the scanner table was brought out and the participant was asked to complete a 12-minute MAST protocol whilst lying on the scanner table: two experimenters (whom the participant had not met yet) acting as "doctors" entered the scanner suite and gave instructions for the MAST task, which involved interleaving blocks of mental arithmetic (counting backward from a four-digit number out loud in steps of 17) and immersing their hand in ice-cold (0-2° Celsius) water. After the MAST, the "doctors" informed the participant that they would continue monitoring their performance from the scanner control room. The table was returned to the scanner and the participant completed another block of the MIST (post-MAST 1). This block was identical to the previous block, providing a direct comparison. In block three of the MIST (post-MAST 2), stress was increased with time pressure and monitoring compared to the implied average on a performance bar. After this block, one "doctor" gave negative verbal feedback over the intercom, stating performance was well below average and to make the data usable the

participant would need to improve in this final block. Then, the participant completed the final block (post-MAST 3), identical to post-MAST 2. The length of the blocks was determined by a computer algorithm (thus, introducing unpredictability and uncontrollability) and the “doctors” provided evaluation of the arithmetic task for a socio-evaluative component; moreover, time pressure was calibrated by participants’ prior responses. Self-report affective ratings were collected pre- and post-stress to confirm the effectiveness of the stress manipulation. Participants were debriefed at the end of the study session.

### ***MRI data acquisition and preprocessing***

Structural data were acquired with a T1-weighted magnetization-prepared rapid acquisition having gradient multi-echo (MPRAGE) imaging sequences with the following acquisition parameters: repetition time (TR) = 2530 ms; echo times (TE) = 1.69, 3.55, 5.41 and 7.27 ms; field of view = 256 mm; voxel dimensions = 1.0 x 1.0 x 1.0 mm<sup>3</sup>; 176 slices. Functional MRI data were acquired using a gradient echo T2\*-weighted echo planar imaging sequence with the following acquisition parameters: repetition time (TR) = 2000 ms; echo time (TE) = 30 ms; field of view = 204 mm; voxel dimension = 1.5 x 1.5 x 1.5 mm; 84 interleaved slices with a multiband acceleration factor of 3.

### ***Anatomical data preprocessing***

The T1-weighted (T1w) images were corrected for intensity non-uniformity (INU) with N4BiasFieldCorrection (7), distributed with ANTs 3.0.0 (8) (RRID:SCR\_004757), and used as T1w-reference throughout the workflow. The T1w-reference was then skull-stripped with a Nipype implementation of the antsBrainExtraction.sh workflow (from ANTs), using OASIS30ANTs as target template. Brain tissue segmentation of cerebrospinal fluid (CSF), white-matter (WM) and gray-matter (GM) was performed on the brain-extracted T1w using fast (FSL 6.0.0, RRID:SCR\_002823 (9)). Brain surfaces were reconstructed using recon-all (FreeSurfer 6.0.1, RRID:SCR\_001847 (10)), and the

brain mask estimated previously was refined with a custom variation of the method to reconcile ANTs-derived and FreeSurfer-derived segmentations of the cortical gray-matter of Mindboggle (RRID:SCR\_002438 (11)). Volume-based spatial normalization to standard space (MNI152Nlin6Asym) was performed through nonlinear registration with antsRegistration (ANTs 3.0.0), using brain-extracted versions of both T1w reference and the T1w template.

### ***Functional data preprocessing***

For each of the four BOLD runs, the following preprocessing was performed. First, a reference volume and its skull-stripped version were generated using a custom methodology of fMRIPrep. A deformation field to correct for susceptibility distortions was estimated based on fMRIPrep's fieldmap-less approach. The deformation field resulted from co-registering the BOLD reference to the same-participant T1w-reference with its intensity inverted (12,13). Registration was performed with antsRegistration (ANTs 3.0.0), and the process regularized by constraining deformation to be nonzero only along the phase-encoding direction and modulated with an average fieldmap template (14). Based on the estimated susceptibility distortion, a corrected EPI (echo-planar imaging) reference was calculated for a more accurate co-registration with the anatomical reference. The BOLD reference was then co-registered to the T1w reference using bbregister (FreeSurfer), which implements boundary-based registration (15). Co-registration was configured with six degrees of freedom. Head-motion parameters with respect to the BOLD reference (transformation matrices, and six corresponding rotation and translation parameters) are estimated before any spatiotemporal filtering using mcflirt (FSL 6.0.0 (16)). BOLD runs were slice-time corrected using 3dTshift from AFNI 20190007 (17) (RRID:SCR\_005927). The BOLD time-series were resampled to surfaces on the following spaces: fsaverage, MNI152Nlin6Asym. The BOLD time-series (including slice-timing correction) were resampled onto their original, native space by applying a single, composite transform to correct for head-motion and susceptibility distortions. These resampled BOLD time-series will be referred to as preprocessed BOLD

in original space, or just preprocessed BOLD. All resamplings can be performed with a single interpolation step by composing all the pertinent transformations (i.e., head-motion transform matrices, susceptibility distortion correction when available, and co-registrations to anatomical and output spaces). Gridded (volumetric) resampling was performed using `antsApplyTransforms` (ANTs), configured with Lanczos interpolation to minimize the smoothing effects of other kernels (18). Non-gridded (surface) resampling was performed using `mri_vol2surf` (FreeSurfer). Several confounding time-series were calculated based on the preprocessed BOLD: framewise displacement (FD), DVARS and three region-wise global signals. FD and DVARS were calculated for each functional run, both using their implementations in Nipype. Frames that exceeded a threshold of 0.5 mm FD or 1.5 standardised DVARS were annotated as motion outliers. Any participant with >20% motion outliers per run was excluded from analysis (1 rMDD excluded all runs, 1 MDD excluded all runs, 2 HC excluded 2 runs, 2 HC excluded 1 run, 2 MDD excluded 1 run, 2 rMDD excluded 1 run). Motion artifacts were estimated using independent component analysis (ICA-AROMA, (19)), visually checked and removed from the preprocessed BOLD on MNI space time-series using FSL's `regfilt`, after removal of non-steady state volumes and spatial smoothing with an isotropic, Gaussian kernel of 6mm FWHM (full-width half-maximum). The BOLD time-series were resampled into standard MNI space using `antsApplyTransforms` (ANTs 3.0.0). Finally, the preprocessed, normalized BOLD runs were temporally filtered using a high bandpass of 150 sec and masked using the standard MNI152Nlin6Asym T1 brain mask.

### ***GABA MRS acquisition and processing***

The T1-weighted structural images were used to place a voxel in the rACC (17.50 ml; 35 x 20 x 25 mm<sup>3</sup>, Figure S1) and left DLPFC (18.75 ml; 25 x 30 x 25 mm<sup>3</sup>, Figure S1) for MRS data collection. The left DLPFC is implicated in MDD, with foundations in frontal asymmetry work and is a target for many established and novel neuromodulation interventions for MDD (e.g. rTMS, tDCS). Indeed, one of the proposed mechanisms of action for neuromodulation is through modification of GABA concentrations

(20,21). As the GABA measurement is before the stressor we were more interested in baseline features of MDD/rMDD and its cortical treatment targets, rather than stress-related effects of the experimental manipulation, which would have been more relevant to right DLPFC.

The MRS voxels were placed manually by the same MRS physicist (Dr. Zuo) using a standard guidance image and landmarks such as the genu of the corpus callosum (for the rACC) and inner table of the calvaria (for the DLPFC). Proton GABA+ (macromolecular-contaminated) measurement employed a MESHcher-GARwood Point RESolved Spectroscopy (MEGA-PRESS) sequence obtained from the University of Minnesota with the acquisition frequency sitting at 3.0ppm and frequency-selective editing pulses, each with a duration of 17ms alternatively at 1.9 ppm (on) and 7.5 ppm (off) interleaved with the averages (22–25). MEGA-PRESS is an established MRS acquisition protocol for GABA detection that has demonstrated superior GABA test-retest reliability compared with other sequences, as described in detail in (26). The magnetic field homogeneity within the prescribed voxel was adjusted using a vendor-provided 3D shimming routine with additional water suppression optimization (completed by the same MRS physicist for all participants (Dr. Zuo)).

GABA+ concentrations are reported as GABA+/water (using water as an external reference, reported in mM), and partial-volume effect (i.e., tissue types in the voxels) was corrected. Water was chosen as the quantitation normalizer instead of the more conventional creatine because brain creatine is an important component in the brain energetic system. Thus, its level is sensitive to several factors, including rates of adenosine triphosphate (ATP) turnover, food intake such as creatine supplements and age (27,28). Also, the stress induction used in this study may have impacted the rate of brain ATP turnover due to increased workload to maintain function under stress. Furthermore, we were not able to control the daily activities or food intake of participants. For these reasons, we chose to use unsuppressed water signal, which was likely a more stable quantity given the study features. The MRS signal is subject to different proton densities, T1 and T2 relaxation times in gray matter (GM), white matter (WM), and cerebrospinal fluid (CSF) (29). Therefore, the volume fractions of different tissue types in our MRS voxel

ROIs have been calculated by segmenting each participant's T1 image in SPM12 and reconstructing the MRS voxels to assess % grey matter. Partial volume effects on metabolite concentrations have been corrected as we described before (30,31). LCModel fitting of the MRS data was assessed for quality based on Cramer-Rao Lower Bound (CRLB) values of <15% and signal-to-noise ratios of >20; additionally, spectra (Figure S1) were visually assessed by MR physicists (Drs. Chen and Du) to exclude anyone with the severe baseline distortions, excluding one participant (final N = 114). GABA MRS data were not acquired for 5 participants (4 HC, 1 rMDD).

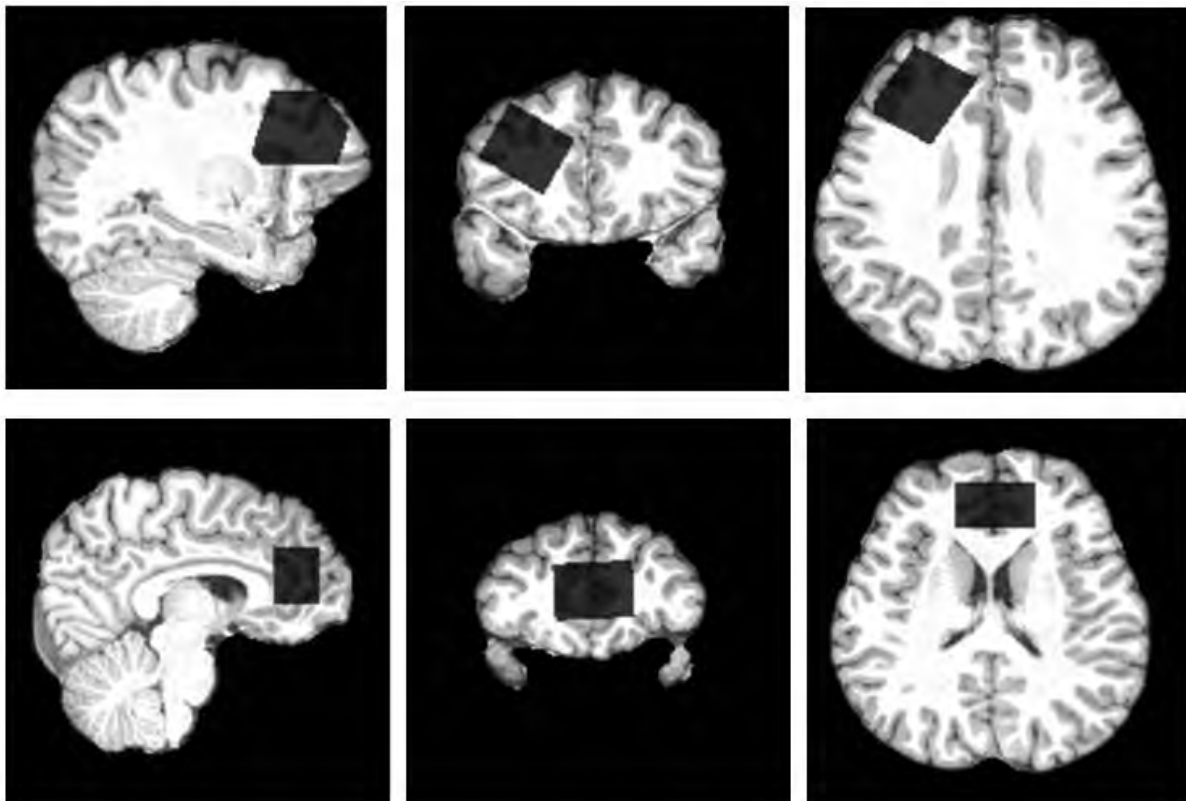


**FIGURE S1.** Images illustrating the voxel placement for the (A) left dorsolateral prefrontal cortex (DLPFC) and (B) rostral anterior cingulate cortex (rACC). Voxel placement is presented in sagittal, coronal, and axial views on a single subject for each region.

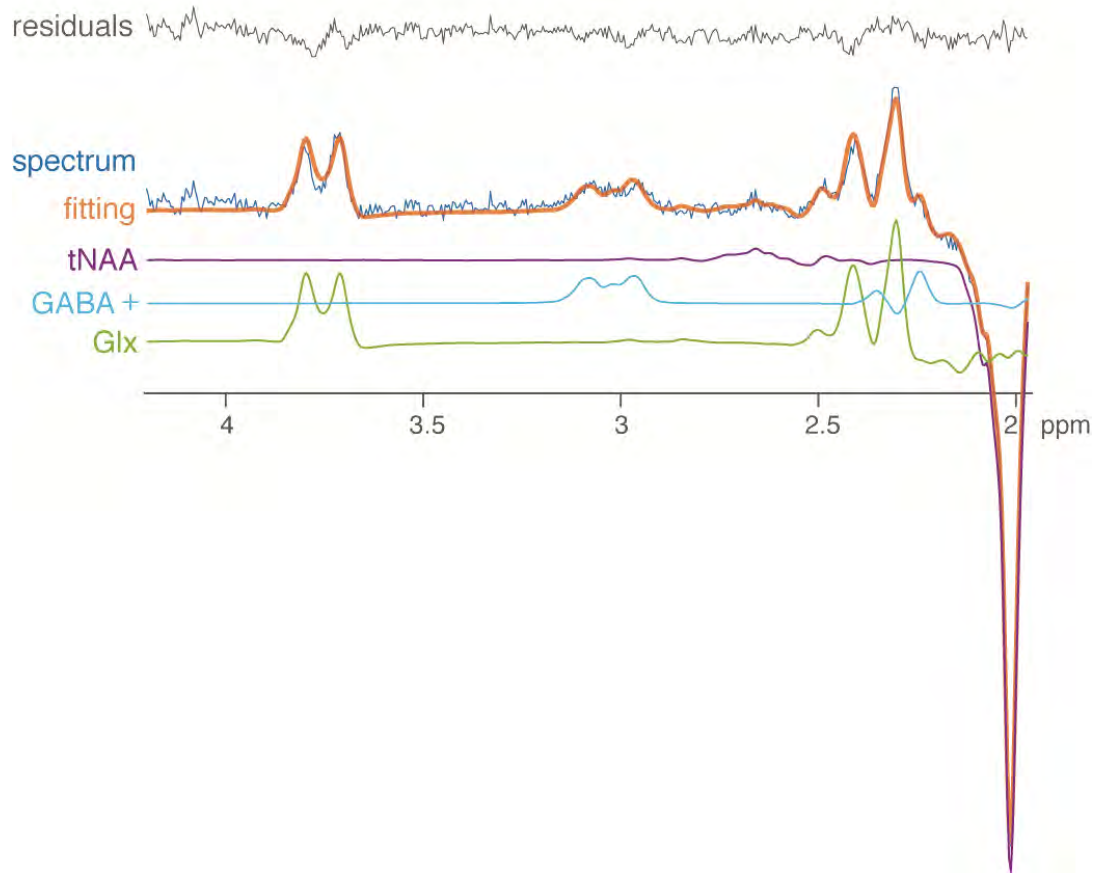


**FIGURE S2.** GABA+-edited (difference) spectrum showing metabolite fitting lines as estimated with LCModel, depicting the GABA+-edited spectrum (dark blue), fitting line (orange), total NAA (tNAA; purple), GABA+ (light blue), glutamate+glutamine (Glx; green), and residuals (grey).

### ***Blood cortisol collection and analysis***

Trained technicians or nurses inserted a saline-lock IV line in the forearm. Blood acquisition commenced 60-80 minutes before participants entered the MRI scanner, with an in-scanner blood draw (baseline) one hour after entering the scanner, after the MRS scan and just prior to the start of the stressor (MAST0). All other blood draws were timed to the beginning of the MAST stressor. A 15-min in-scanner blood sample was drawn after the completion of the stressor (MAST15), followed by a 30-min in-scanner blood draw (MAST30) and 60-min (MAST60) and 90-min (MAST90) blood draws, out-of-scanner in a quiet room. Three additional blood draws occurred outside the scanner for a separate task to be published elsewhere.

Subjects remained inside the bore of the magnet during in-scanner blood draws. The timing of these blood draws was based on the expected peak response (following the onset of the stressor) of cortisol between 10 and 60 min after stress onset. Hormonal data were missing or not reported for some subjects due to gaps in nursing coverage, or poor IV access preventing blood acquisition during scanning (10 HC; 13 MDD, 10 rMDD). For those with partial data, when MAST0 and at least one other timepoint were available, missing timepoints were imputed using mixed-models regression. Approximately 5-20 mL of blood was sampled at each time point, allowed to clot for 30 min, spun in a refrigerated centrifuge, aliquoted, and stored frozen at -80°C. Cortisol was analyzed in duplicate with a commercial immunoassay kit (0.04 ug/dL; 4.4–6.7%; Immunoradiometric Assay (IRMA), DiaSorin, Inc., Stillwater, MN). Blood cortisol changes from stress were quantified using area under the curve (AUC) calculations (32). Area under the curve with respect to ground (AUCg) estimates the magnitude of the cortisol response overall and area under the curve with respect to increase from baseline (AUCi) estimates the magnitude of the cortisol response from an individual's baseline. Due to gaps in nurses' coverage and difficulty obtaining blood, 33 participants (10 HC, 13, MDD, 10 rMDD) did not have cortisol AUCi measurements.

### ***Network Maps***

We ran a group ICA of the task fMRI data; this step temporally concatenated all runs and participants using MELODIC in FSL. Following our recent work, we selected model order 40 group ICA results for analyses. Based on Menon's triple network model (33) and regions of interest for stress tasks (34), *a priori* task networks of interest were: 1) right frontoparietal control network (FPN; main text Figure 2A); 2) a stress-related ventromedial prefrontal, striatal, anterior cingulate cortex network (vmPFC-Str-ACC; Figure 2B); 3) salience network (Figure 2C); 4) a second stress-related network including temporal regions, the insula, and amygdala (Temp-Ins-Amyg; Figure 2D); and 5) the default mode network (DMN; Figure 2E). A maximum of 5 networks were selected to reduce multiple comparisons. Seminal work comparing functional activation between task and rest (35) showed that the right FPN corresponded with

perception–somesthesis–pain, whereas the left FPN corresponded with cognition-language. Therefore, although the left FPN was among the 40 components for the group ICA, to limit the number of comparisons, we selected the right FPN for stress-related activation because we thought this would be the most likely of the two to show stress-related activation following our manipulation.

### ***Independent component analysis of functional data***

The set of five spatial maps (main text Figure 2) from the group-average analysis were used to generate participant-specific versions of the spatial maps, and associated timeseries, using dual regression (36,37). First, for each participant, the full set of independent component (IC) maps was regressed (as spatial regressors in a multivariate regression) into the participant's 4D task fMRI dataset. This resulted in a set of participant-specific time series, one per group IC spatial map. Next, those timeseries were regressed (as temporal regressors, again in a multiple regression) into the same 4D dataset, resulting in a set of participant-specific spatial maps, one per group-level spatial map. We then tested for within- and between-group differences using network modeling (38). First, we used the participant-specific timeseries from dual regression to create between-network connectivity matrices for each pair of networks using FSLNETS v0.6 (39) with non-aggressive removal of other network effects. To control for collinearity between the networks, we estimated partial correlation coefficients via Ridge Regression (with  $\rho = 0.01$ ) in FSLNets. Partial correlation r-values were converted to z-statistics with Fisher's transformation (38). Network amplitude (how much a given network deviates from its own mean) was also estimated for each of the networks of interest, using the diagonal of the covariance matrix.

### ***Network modelling and statistical analysis***

For repeated measures (main outcome network variables, self-report), mixed effects regressions were conducted using the lmerTest package in R (40), a method that efficiently handles non-independence of repeated measures. GABA+ and cortisol AUC<sub>i</sub> outliers were determined by Cook's Distance for the group × sex linear model, with a standard cut off of 4/N.

### **Supplemental Results**

#### ***Affective Ratings***

Group differences in affective response to stress (post-pre) were analyzed using linear regression for state anxiety (STAI-S), positive and negative affect and visual analogue scales with a between-subjects factors of group (HC, MDD, rMDD) and sex (male, female). For all affective rating measures there were significant main effects of stress (Figure S3), indicating that the stressor increased negative affect and decreased positive affect across participants. After Bonferroni correction there was a trend group \* sex interaction on hostility ratings (uncorrected  $p=0.02$ ), with the female MDD group showing greater hostility changes from stress than the male MDD group. There was also a trend group \* sex interaction on positive affect (uncorrected  $p=0.03$ ), driven by the female rMDD group showing greater decreases in positive affect from stress than the male MDD group. As the difficulty of the MIST is set high to induce stress, accuracy in the MIST task typically reaches a floor and therefore is not analyzed.

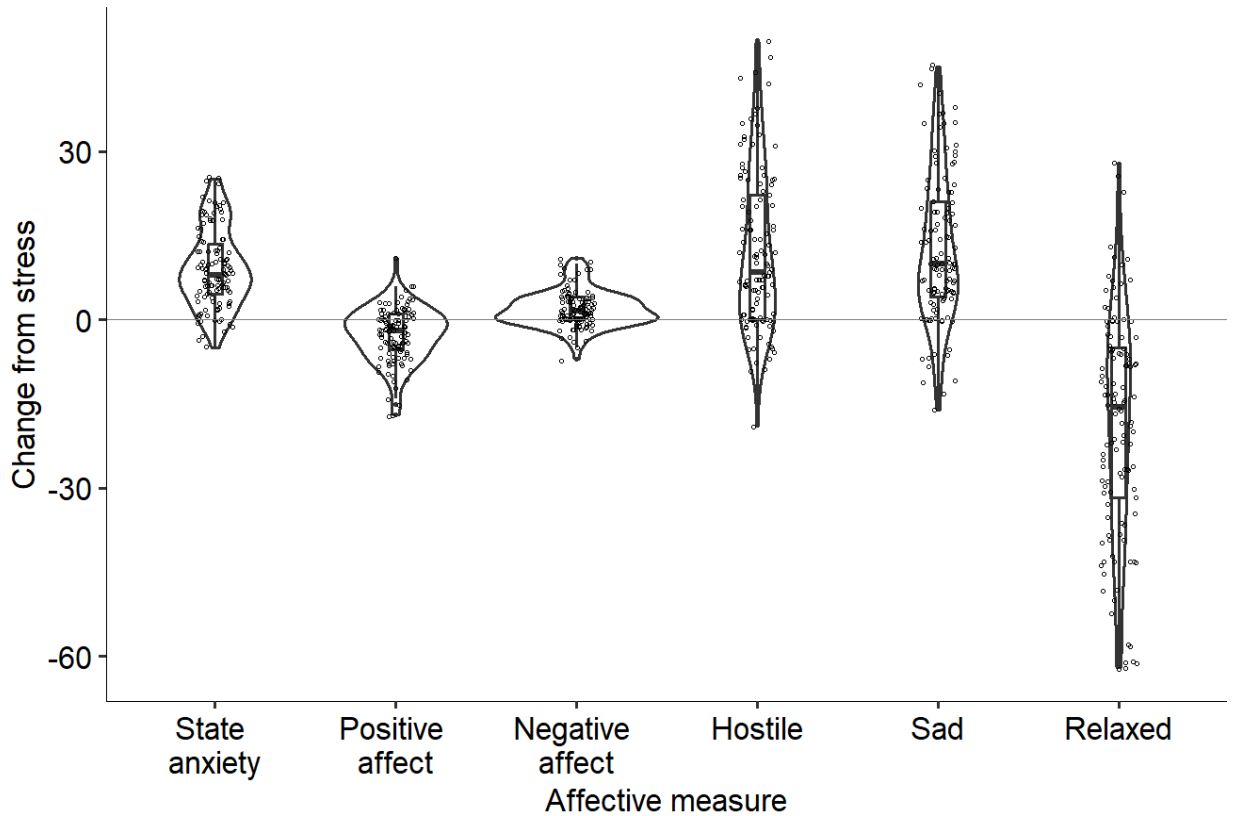


**FIGURE S3. Affective rating changes from stress**

### ***GABA MRS***

There were no significant effects of group, sex or their interaction in DLPFC GABA (all  $p > 0.06$ ).

Across all participants, rACC GABA+ showed a trend positive correlation with rACC gray matter (GM) ( $r(103) = 0.18, p = 0.06$ ) whereas DLPFC GABA+ showed a significant negative correlation ( $r(108) = -0.21, p = 0.03$ ). When evaluating healthy controls only the rACC correlation strengthened ( $r(30) = 0.44, p = 0.01$ ) but the DLPFC correlation lost significance ( $r(30) = -0.18, p = 0.33$ ). To further explore potential factors affecting the relationship between GABA+ and GM, we fit linear models for both GABA+ voxels predicting GABA+ by GM\*group\*sex. There were no significant interactions of GM with group or sex (all  $p > 0.16$ ).

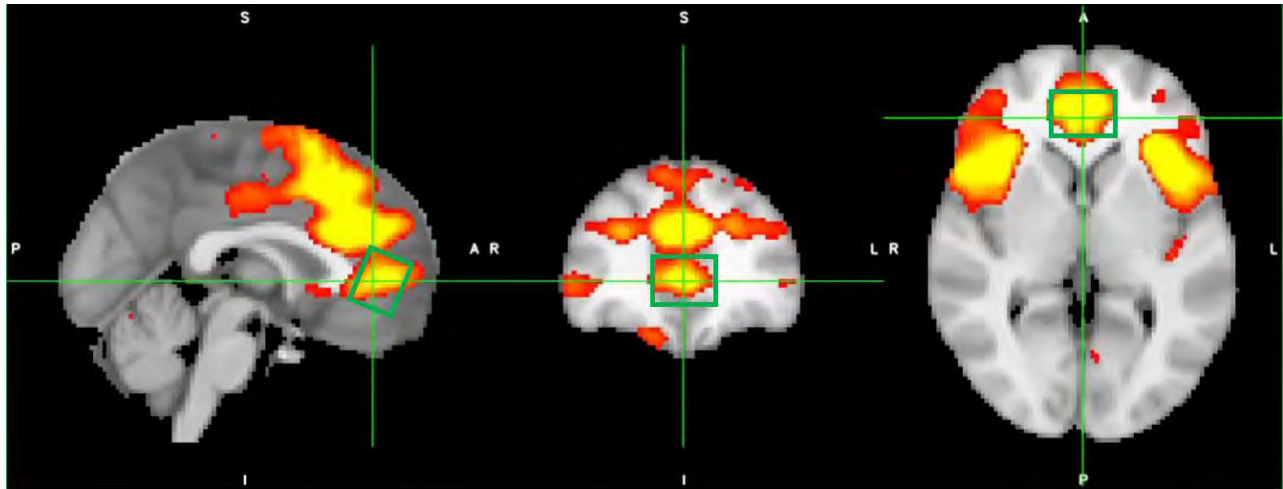


**FIGURE S4.** Overlap between Salience network and approximate location of rostral anterior cingulate MRS voxel ( $35 \times 20 \times 25 \text{ mm}^3$ )

*Dimensional relationships between GABA and stress-related changes in cortisol, circuitry and affect*

To aid interpretation and investigate further relationships between our multiple measures, correlational analyses were run across all participants relating GABA+ and all significant *stress-related-changes* in networks, cortisol and affective ratings. See Figure S5 for all significant associations.

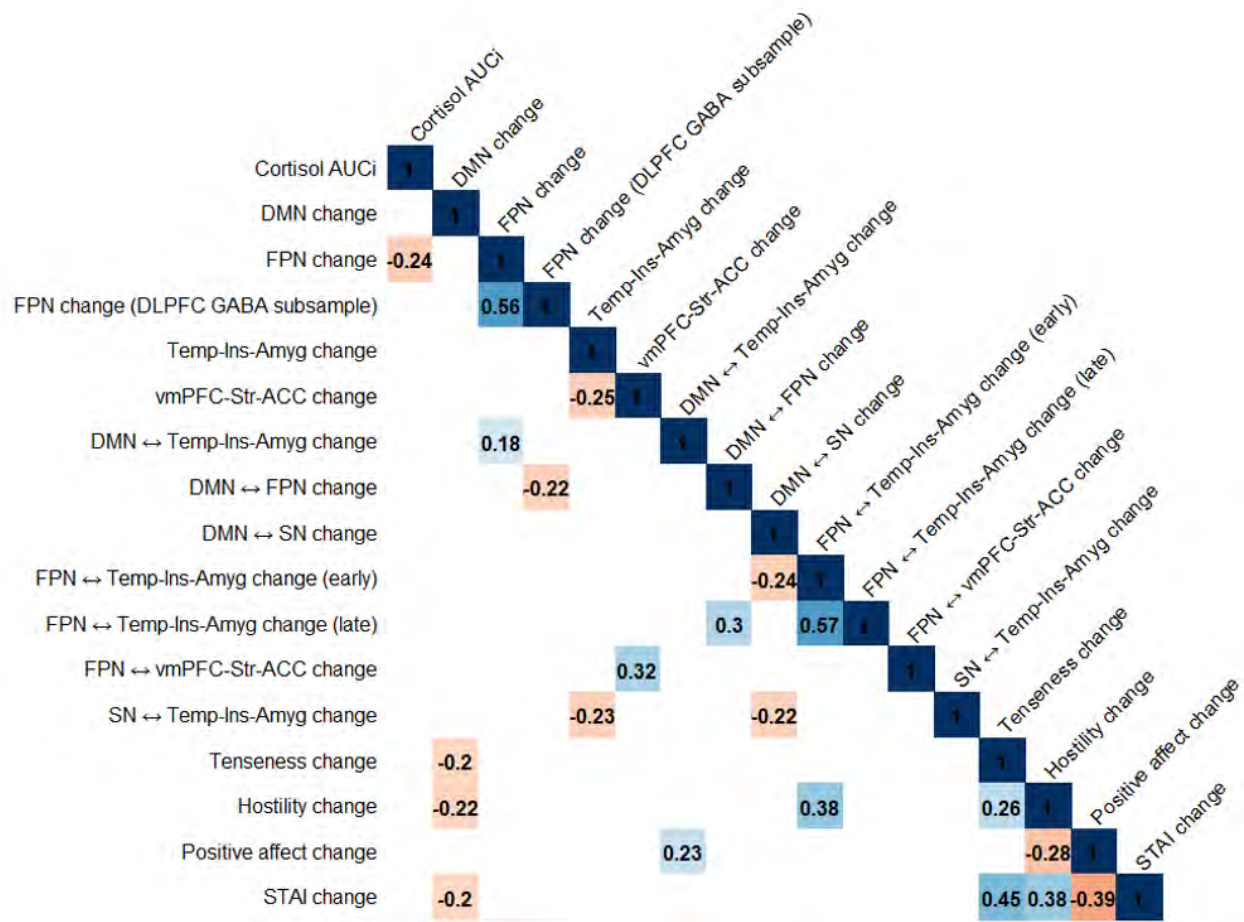


**FIGURE S5: Significant associations between stress-related changes in cortisol, networks and affect.** Correlation plot shows only significant correlations ( $p < 0.05$ , uncorrected). FPN: Right frontoparietal network; vmPFC-Str-ACC: Ventromedial prefrontal cortex, ventral striatum and anterior cingulate cortex; SN: Salience network; Temp-Ins-Amyg: Temporal-insula-amygdala network; DMN: Default mode network; STAI: Spielberger State Trait Anxiety Inventory – state. Coefficient shown is Pearson’s  $r$ . These measures are meant to be exploratory and would not all survive correction for multiple comparisons.

Across all participants, the *stress-related* increase in vmPFC-Str-ACC amplitude was associated with *stress-related* decreases in Temp-Ins-Amyg amplitude ( $r(112) = -0.25, p = 0.008$ ) and *stress-related* increases in FPN ↔ vmPFC-Str-ACC connectivity ( $r(94) = 0.32, p = 0.001$ ), suggesting further potential between network interdependencies over the course of the stressor. Moreover, the stress-related decrease

in DMN amplitude was associated with increased ratings of hostility ( $r(100)=-0.22, p=0.03$ ), tenseness ( $r(102)=-0.20, p=0.04$ ) and state-anxiety ( $r(100)=-0.20, p=0.04$ ), suggesting a potential relationship between increases in negative affect and decreases in DMN amplitude from stress. The *stress-related* decrease in FPN amplitude was associated with cortisol AUCi ( $r(84)=-0.24, p=0.02$ ) and *stress-related* reductions in DMN↔Temp-Ins-Amyg connectivity ( $r(117)=0.18, p=0.05$ ), suggesting that greater cortisol is associated with reduced engagement of the FPN.

The DLPFC GABA-related decrease in overall FPN amplitude was associated with *stress-related* increases in FPN↔DMN connectivity ( $r(94)=-0.22, p=0.03$ ) suggesting a potential relationship between reduced top-down activation overall and increased top-down control of self-referential networks. The group and cortisol-related changes in FPN↔Temp-Ins-Amyg connectivity were also associated with increased ratings of hostility ( $r(74)=0.38, p<0.001$ ), positively associated with *stress-related* change in FPN↔DMN connectivity ( $r(84)=0.29, p=0.007$ ) and negatively associated with *stress-related* change in DMN↔SN connectivity ( $r(79)=-0.27, p=0.03$ ), suggesting that *stress-related* increased in top-down connectivity between the FPN and a stress task network and self-referential network could be associated with reductions in evaluative/self-referential connectivity. Potentially linked to this, the sex- and cortisol-related changes in SN↔Temp-Ins-Amyg connectivity were also negatively associated with *stress-related* change in DMN↔SN connectivity ( $r(79)=-0.24, p=0.05$ ), suggesting that increased evaluation of the stress signals may result in less evaluation of self-referential thoughts.

### **Sensitivity Analysis of Power**

Sensitivity analyses based on 1000 Monte Carlo simulations of the data from the FPN network were carried out using the *simr* package in R to determine the smallest effect size that was detectable at 80% power. For the main effect of *group* (follow-up contrast of MDD vs. HC), the 95% confidence interval (CI) to detect an effect size (beta) of 0.12 was 76.65-81.77. For the main effect of *stress* (follow-up contrast of post-MAST 2 vs. baseline), the 95% CI to detect an effect size (beta) of 0.09 was 75.72-80.91.

For the *group \* stress* interaction (follow-up contrast of run2H vs. baseline, MDD vs. HC) the 95% CI to detect an effect size (beta) of 0.13 was 77.49 - 82.53. For the *sex \* group* interaction (follow-up contrast of Female vs. Male, MDD vs. HC) the 95% CI to detect an effect size (beta) of 0.25 was 77.18 - 82.25. For the *sex \* group \* stress* interaction (follow-up contrast of Female vs. Male, MDD vs. HC run2H vs. baseline) the 95% CI to detect an effect size (beta) of 0.25 was 75.93 - 81.10.

**TABLE S1. Demographics and Clinical Scores – All participants.** BDI: Beck Depression Inventory; HDRS: Hamilton Depression Rating Scale; STAI-T: State-Trait Anxiety Inventory – Trait anxiety, QIDS: Quick Inventory of Depressive Symptomatology, MASQ: Mood and Anxiety Symptom Questionnaire, rACC: rostral anterior cingulate cortex, DLPFC: dorsolateral prefrontal cortex

Measure	HC	MDD	rMDD	Three group comparison	MDD v rMDD
<b>N</b>	44	44	42		
<b>Female</b>	21	22	22	F(2,127) = 0.09, <i>p</i> = 0.9	t(84) = 0.21, <i>p</i> = 0.8
<b>Age</b>	21.36 (2.30)	20.84 (2.12)	21.59 (1.98)	F(2,127) = 1.40, <i>p</i> = 0.2	t(84) = 1.70, <i>p</i> = 0.1
<b>Years of Education</b>	15.09 (2.27)	14.41 (1.84)	15.02 (1.51)	F(2,123) = 1.63, <i>p</i> = 0.2	t(81) = 1.33, <i>p</i> = 0.1
<b>Race: Asian (n)</b>	12	7	5		
<b>Race: Black (n)</b>	5	5	2		
<b>Race: White (n)</b>	22	25	28		
<b>Race: Native Hawaiian (n)</b>	0	0	1		
<b>Race: Multi-racial (n)</b>	4	3	5		
<b>Race: Unknown (n)</b>	1	4	1		
<b>BDI (mean, median, interquartile range IQR)</b>	0.32, 0 (0-0)	28.92, 29 (25-33)	1.37, 1 (0-2)	<b>H(3) = 83, <i>p</i> &lt; 0.001</b>	<b>W = 1369, <i>p</i> &lt; 0.001</b>
<b>Hamilton Depression Rating Scale (mean, median, IQR)</b>	0.35, 0 (0-0)	16.43, 16 (14-19)	1.17, 1 (0-2)	<b>H(3) = 83, <i>p</i> &lt; 0.001</b>	<b>W = 1443, <i>p</i> &lt; 0.001</b>
<b>Trait Anxiety (STAI-T) (mean, SD)</b>	26.34 (4.30)	61.47 (7.59)	33.31 (7.51)	<b>F(2,112) = 297.32, <i>p</i> &lt; 0.001</b>	<b>t(75) = 16.36, <i>p</i> &lt; 0.001</b>
<b>QIDS (mean, median, IQR)</b>	0.43, 0 (0-1)	14, 13 (12-16.5)	0.71, 0 (0-1)	<b>H(3) = 67, <i>p</i> &lt; 0.001</b>	<b>W = 1026, <i>p</i> &lt; 0.001</b>
<b>Snaith-Hamilton Pleasure Scale (mean, SD)</b>	20.76 (5.78)	35.05 (5.92)	21.49 (5.42)	<b>F(2,111) = 76.33, <i>p</i> &lt; 0.001</b>	<b>t(74) = 10.42, <i>p</i> &lt; 0.001</b>
<b>MASQ - Anxious Arousal (mean, median, IQR)</b>	17.47, 17 (17-18)	29.18, 25.5 (22.25-34)	18.06, 17 (17-18.25)	<b>H(3) = 57, <i>p</i> &lt; 0.001</b>	<b>W = 1229, <i>p</i> &lt; 0.001</b>
<b>MASQ - General Distress (Anxious) (mean, median, IQR)</b>	12.21, 12 (11-13)	26.05, 24 (18-33)	13.34, 13 (11.25-14)	<b>H(3) = 65, <i>p</i> &lt; 0.001</b>	<b>W = 1368, <i>p</i> &lt; 0.001</b>
<b>MASQ - General Distress (Depression) (mean, median, IQR)</b>	12.21, 12 (12-13)	41.90, 43 (35-48.5)	14.36, 13.5 (12-17)	<b>H(3) = 83, <i>p</i> &lt; 0.001</b>	<b>W = 1404, <i>p</i> &lt; 0.001</b>
<b>MASQ - Anhedonic Depression (mean, median, IQR)</b>	44.86, 42 (36-54)	85.72, 86 (80-92)	52.00, 50 (44-62)	<b>H(3) = 73, <i>p</i> &lt; 0.001</b>	<b>W = 1317, <i>p</i> &lt; 0.001</b>
<b>Number of MDD episodes (mean, median, IQR)</b>	-	2 (1-3)	1 (1-2)		<b>W = 1230, <i>p</i> = 0.004</b>
<b>Age of first MDD onset (mean, SD)</b>	-	16.84 (3.49)	17.61 (2.40)		t(76) = 1.19, <i>p</i> = 0.2
<b>AUCi (mean, SD)</b>	174 (255)	97.7 (230)	371 (258)		
<b>rACC GABA (mean, SD)</b>	1.19 (0.16)	1.10 (0.13)	1.10 (0.16)		
<b>DLPFC GABA (mean, SD)</b>	1.05 (0.13)	1.06 (0.11)	1.08 (0.10)		
<b>AUCi outliers</b>	2	2	4		
<b>rACC GABA outliers</b>	2	3	0		
<b>DLPFC GABA outliers</b>	2	3	0		

**TABLE S2. Demographics and Clinical Scores – Participants with blood collected.** BDI: Beck Depression Inventory; HDRS: Hamilton Depression Rating Scale; STAI-T: State-Trait Anxiety Inventory – Trait anxiety, QIDS: Quick Inventory of Depressive Symptomatology, MASQ: Mood and Anxiety Symptom Questionnaire, rACC: rostral anterior cingulate cortex, DLPFC: dorsolateral prefrontal cortex

Measure	HC	MDD	rMDD	Three group comparison	MDD v rMDD
<b>N</b>	32	29	28		
<b>Female</b>	13	16	14	F(2,86) = 0.66, <i>p</i> = 0.5	t(55) = 0.38, <i>p</i> = 0.7
<b>Age</b>	21.22 (2.31)	20.62 (1.87)	21.54(2.12)	F(2,86) = 1.38, <i>p</i> = 0.3	t(54) = 1.72, <i>p</i> = 0.1
<b>Years of Education</b>	14.9 (2.17)	14.31 (1.65)	14.85(1.33)	F(2,86) = 1.01, <i>p</i> = 0.4	t(53) = 1.38, <i>p</i> = 0.2
<b>Race: Asian (n)</b>	8	4	4		
<b>Race: Black (n)</b>	1	2	1		
<b>Race: White (n)</b>	18	17	18		
<b>Race: Native Hawaiian (n)</b>	0	0	0		
<b>Race: Multi-racial (n)</b>	4	2	4		
<b>Race: Unknown (n)</b>	1	4	1		
<b>BDI (mean, median, interquartile range IQR)</b>	0.17, 0, (0-0)	27.48, 28 (23-33)	1.21, 1 (0-2)	<b>H(3) = 58, <i>p</i> &lt; 0.001</b>	<b>W = 552, <i>p</i> &lt; 0.001</b>
<b>Hamilton Depression Rating Scale (mean, median, IQR)</b>	0.32, 0, (0-0)	16.82, 16 (14-20)	1.16, 0.5 (0-1.75)	<b>H(3) = 54, <i>p</i> &lt; 0.001</b>	<b>W = 572, <i>p</i> &lt; 0.001</b>
<b>Trait Anxiety (STAI-T) (mean, SD)</b>	25.93 (3.68)	61.29 (7.86)	33 (8.09)	<b>F(2,76) = 196.98, <i>p</i> &lt; 0.001</b>	<b>t(48) = 12.53, <i>p</i> &lt; 0.001</b>
<b>QIDS (mean, median, IQR)</b>	0.42, 0 (0-0)	13.5, 13 (12-14)	0.69, 0 (0-1)	<b>H(3) = 48, <i>p</i> &lt; 0.001</b>	<b>W = 494, <i>p</i> &lt; 0.001</b>
<b>Snaith-Hamilton Pleasure Scale (mean, SD)</b>	20.51 (5.38)	35.08 (5.84)	21.72 (5.39)	<b>F(2,75) = 53.67, <i>p</i> &lt; 0.001</b>	<b>t(46) = 8.31, <i>p</i> &lt; 0.001</b>
<b>MASQ - Anxious Arousal (mean, median, IQR)</b>	17.48, 17 (17-18)	27.74, 24 (22-32)	18.08, 17 (17-18)	<b>H(3) = 42, <i>p</i> &lt; 0.001</b>	<b>W = 533, <i>p</i> &lt; 0.001</b>
<b>MASQ - General Distress (Anxious) (mean, median, IQR)</b>	12.24, 12 (11-12)	25.83, 24 (18-33)	13.5, 13 (12-14)	<b>H(3) = 44, <i>p</i> &lt; 0.001</b>	<b>W = 580, <i>p</i> &lt; 0.001</b>
<b>MASQ - General Distress (Depression) (mean, median, IQR)</b>	12.57, 12 (12-13)	40.21, 40.5 (33.75-45.5)	13.84, 13 (12-15)	<b>H(3) = 55, <i>p</i> &lt; 0.001</b>	<b>W = 600, <i>p</i> &lt; 0.001</b>
<b>MASQ - Anhedonic Depression (mean, median, IQR)</b>	44.93, 42 (35-54)	84.37, 85 (80-91.5)	52.24, 48 (42-64)	<b>H(3) = 46, <i>p</i> &lt; 0.001</b>	<b>W = 542, <i>p</i> &lt; 0.001</b>
<b>Number of MDD episodes (mean, median, IQR)</b>		2 (1-3)	1 (1-1.25)		<b>W = 598, <i>p</i> &lt; 0.001</b>
<b>Age of first MDD onset (mean, SD)</b>		16.38 (3.5)	17.75 (2.08)		t(46) = 1.80, <i>p</i> = 0.1

**TABLE S3. Study Sample size for each measure**

HC: Healthy control; MDD: Current major depressive disorder; rMDD: remitted major depressive disorder.

<b>Group</b>	<b>fMRI data</b>	<b>rACC GABA+</b>	<b>DLPFC GABA+</b>	<b>Cortisol</b>
HC (N)	42	30	30	32
MDD (N)	41	37	41	29
rMDD (N)	41	36	38	28
<b>Total</b>	<b>124</b>	<b>103</b>	<b>109</b>	<b>89</b>

**TABLE S4. Mixed effects models**

<b>Dependent variable (network(s) of interest) and tests evaluated</b>	<b>Mixed effects model</b>
Default mode network (DMN) <i>(1) stress, (2) group, (3) sex, (4) group × sex, (5) sex × stress, (6) group × stress, (7) group × sex × stress, (8-10) group × sex × stress × cortisol/ rACC GABA/DLPFC GABA, (11-13) sex × stress × cortisol/ rACC GABA/DLPFC GABA, (14-16) group × stress × cortisol/ rACC GABA/DLPFC GABA, (17-19) stress × cortisol/ rACC GABA/DLPFC GABA</i>	DMN_A ~ group × sex × run + (1 subject)
	DMN_A ~ group × sex × run × cortisol_AUCi + (1 subject)
	DMN_A ~ group × sex × run × rACC_GABA + (1 subject)
	DMN_A ~ group × sex × run × DLPFC_GABA + (1 subject)
Frontoparietal network (FPN) amplitude <i>(1) stress, (2) group, (3) group × stress, (4-6) group × stress × cortisol/ rACC GABA/DLPFC GABA, (7-9) stress × cortisol/ rACC GABA/DLPFC GABA</i>	FPN_A ~ group × sex × run + (1 subject)
	FPN_A ~ group × sex × run × cortisol_AUCi + (1 subject)
	FPN_A ~ group × sex × run × rACC_GABA + (1 subject)
	FPN_A ~ group × sex × run × DLPFC_GABA + (1 subject)
Salience network (SN) amplitude	SN_A ~ group × sex × run + (1 subject)

<i>(1) stress, (2) group, (3) group × stress, (4-6) group × stress × cortisol/ rACC GABA/DLPFC GABA, (7-9) stress × cortisol/ rACC GABA/DLPFC GABA</i>	SN_A ~ group × sex × run × cortisol_AUCi + (1 subject)
	SN_A ~ group × sex × run × rACC_GABA + (1 subject)
	SN_A ~ group × sex × run × DLPFC_GABA + (1 subject)
Ventromedial prefrontal cortex – striatal – anterior cingulate cortex network (vmPFC-Str-ACC) network amplitude  <i>(1) stress, (2) group, (3) group × stress, (4-6) group × stress × cortisol/ rACC GABA/DLPFC GABA, (7-9) stress × cortisol/ rACC GABA/DLPFC GABA</i>	vmPFC-Str-ACC_A ~ group × sex × run + (1 subject)
	vmPFC-Str-ACC_A ~ group × sex × run × cortisol_AUCi + (1 subject)
	vmPFC-Str-ACC_A ~ group × sex × run × rACC_GABA + (1 subject)
	vmPFC-Str-ACC_A ~ group × sex × run × DLPFC_GABA + (1 subject)
Temporal – insula – amygdala (Temp-Ins-Amyg) network amplitude  <i>(1) stress, (2) group, (3) group × stress, (4-6) group × stress × cortisol/ rACC GABA/DLPFC GABA, (7-9) stress × cortisol/ rACC GABA/DLPFC GABA</i>	Temp-Ins-Amyg_A ~ group × sex × run + (1 subject)
	Temp-Ins-Amyg_A ~ group × sex × run × cortisol_AUCi + (1 subject)
	Temp-Ins-Amyg_A ~ group × sex × run × rACC_GABA + (1 subject)
	Temp-Ins-Amyg_A ~ group × sex × run × DLPFC_GABA + (1 subject)
DMN x FPN connectivity  <i>(1) stress, (2) group, (3) group × stress, (4-6) group × stress × cortisol/ rACC GABA/DLPFC GABA, (7-9) stress × cortisol/ rACC GABA/DLPFC GABA</i>	DMN x FPN ~ group × sex × run + (1 subject)
	DMN x FPN ~ group × sex × run × cortisol_AUCi + (1 subject)
	DMN x FPN ~ group × sex × run × rACC_GABA + (1 subject)
	DMN x FPN ~ group × sex × run × DLPFC_GABA + (1 subject)
DMN x SN connectivity  <i>(1) stress, (2) group, (3) group × stress, (4-6) group × stress × cortisol/ rACC GABA/DLPFC GABA, (7-9) stress × cortisol/ rACC GABA/DLPFC GABA</i>	DMN x SN ~ group × sex × run + (1 subject)
	DMN x SN ~ group × sex × run × cortisol_AUCi + (1 subject)
	DMN x SN ~ group × sex × run × rACC_GABA + (1 subject)
	DMN x SN ~ group × sex × run × DLPFC_GABA + (1 subject)
DMN x vmPFC-Str-ACC connectivity  <i>(1) stress, (2) group, (3) group × stress, (4-6) group × stress × cortisol/ rACC GABA/DLPFC GABA, (7-9) stress × cortisol/ rACC GABA/DLPFC GABA</i>	DMN x vmPFC-Str-ACC ~ group × sex × run + (1 subject)
	DMN x vmPFC-Str-ACC ~ group × sex × run × cortisol_AUCi + (1 subject)
	DMN x vmPFC-Str-ACC ~ group × sex × run × rACC_GABA + (1 subject)
	DMN x vmPFC-Str-ACC ~ group × sex × run × DLPFC_GABA + (1 subject)
DMN x TIA connectivity	DMN x Temp-Ins Amyg ~ group × sex × run + (1 subject)

<i>(1) stress, (2) group, (3) group × stress, (4-6) group × stress × cortisol/ rACC GABA/DLPFC GABA, (7-9) stress × cortisol/ rACC GABA/DLPFC GABA</i>	DMN x Temp-Ins Amyg ~ group × sex × run × cortisol_AUCi + (1 subject)
	DMN x Temp-Ins Amyg ~ group × sex × run × rACC_GABA + (1 subject)
	DMN x Temp-Ins Amyg ~ group × sex × run × DLPFC_GABA + (1 subject)
FPN x SN connectivity <i>(1) stress, (2) group, (3) group × stress, (4-6) group × stress × cortisol/ rACC GABA/DLPFC GABA, (7-9) stress × cortisol/ rACC GABA/DLPFC GABA</i>	FPN x SN ~ group × sex × run + (1 subject)
	FPN x SN ~ group × sex × run × cortisol_AUCi + (1 subject)
	FPN x SN ~ group × sex × run × rACC_GABA + (1 subject)
	FPN x SN ~ group × sex × run × DLPFC_GABA + (1 subject)
FPN x vmPFC-Str-ACC connectivity <i>(1) stress, (2) group, (3) group × stress, (4-6) group × stress × cortisol/ rACC GABA/DLPFC GABA, (7-9) stress × cortisol/ rACC GABA/DLPFC GABA</i>	FPN x vmPFC-Str-ACC ~ group × sex × run + (1 subject)
	FPN x vmPFC-Str-ACC ~ group × sex × run × cortisol_AUCi + (1 subject)
	FPN x vmPFC-Str-ACC ~ group × sex × run × rACC_GABA + (1 subject)
	FPN x vmPFC-Str-ACC ~ group × sex × run × DLPFC_GABA + (1 subject)
FPN x Temp-Ins Amyg connectivity <i>(1) stress, (2) group, (3) group × stress, (4-6) group × stress × cortisol/ rACC GABA/DLPFC GABA, (7-9) stress × cortisol/ rACC GABA/DLPFC GABA</i>	FPN x Temp-Ins Amyg ~ group × sex × run + (1 subject)
	FPN x Temp-Ins Amyg ~ group × sex × run × cortisol_AUCi + (1 subject)
	FPN x Temp-Ins Amyg ~ group × sex × run × rACC_GABA + (1 subject)
	FPN x Temp-Ins Amyg ~ group × sex × run × DLPFC_GABA + (1 subject)
SN x vmPFC-Str-ACC connectivity <i>(1) stress, (2) group, (3) group × stress, (4-6) group × stress × cortisol/ rACC GABA/DLPFC GABA, (7-9) stress × cortisol/ rACC GABA/DLPFC GABA</i>	SN x vmPFC-Str-ACC ~ group × sex × run + (1 subject)
	SN x vmPFC-Str-ACC ~ group × sex × run × cortisol_AUCi + (1 subject)
	SN x vmPFC-Str-ACC ~ group × sex × run × rACC_GABA + (1 subject)
	SN x vmPFC-Str-ACC ~ group × sex × run × DLPFC_GABA + (1 subject)
SN x Temp-Ins Amyg connectivity <i>(1) stress, (2) group, (3) group × stress, (4-6) group × stress × cortisol/ rACC GABA/DLPFC GABA, (7-9) stress × cortisol/ rACC GABA/DLPFC GABA</i>	SN x Temp-Ins Amyg ~ group × sex × run + (1 subject)
	SN x Temp-Ins Amyg ~ group × sex × run × cortisol_AUCi + (1 subject)
	SN x Temp-Ins Amyg ~ group × sex × run × rACC_GABA + (1 subject)
	SN x Temp-Ins Amyg ~ group × sex × run × DLPFC_GABA + (1 subject)
	vmPFC-Str-ACC x Temp-Ins Amyg ~ group × sex × run + (1 subject)

vmPFC-Str-ACC x Temp-Ins Amyg connectivity (1) stress, (2) group, (3) group × stress, (4-6) group × stress × cortisol/ rACC GABA/DLPFC GABA, (7-9) stress × cortisol/ rACC GABA/DLPFC GABA	vmPFC-Str-ACC x Temp-Ins Amyg ~ group × sex × run × cortisol_AUCi + (1 subject)
	vmPFC-Str-ACC x Temp-Ins Amyg ~ group × sex × run × rACC_GABA + (1 subject)
	vmPFC-Str-ACC x Temp-Ins Amyg ~ group × sex × run × DLPFC_GABA + (1 subject)

## References

1. First MB. Structured clinical interview for the DSM (SCID). *Encycl Clin Psychol*. 2014;1–6.
2. Hamilton M. A rating scale for depression. *J Neurol Neurosurg Psychiatry*. 1960;23(1):56.
3. Rush AJ, Trivedi MH, Ibrahim HM, Carmody TJ, Arnow B, Klein DN, et al. The 16-item quick inventory of depressive symptomatology (QIDS), clinician rating (QIDS-C), and self-report (QIDS-SR): A psychometric evaluation in patients with chronic major depression. *Biol Psychiatry*. 2003;54(5):573–83.
4. Miller R, Stalder T, Jarczok M, Almeida DM, Badrick E, Bartels M, et al. The CIRCORT database: Reference ranges and seasonal changes in diurnal salivary cortisol derived from a meta-dataset comprised of 15 field studies. *Psychoneuroendocrinology*. 2016;73:16–23.
5. Dedovic K, Renwick R, Mahani NK, Engert V, Lupien SJ, Pruessner JC. The Montreal Imaging Stress Task: using functional imaging to investigate the effects of perceiving and processing psychosocial stress in the human brain. *J Psychiatry Neurosci*. 2005;30(5):319–25.
6. Smeets T, Cornelisse S, Quaedflieg CWEM, Meyer T, Jelicic M, Merckelbach H. Introducing the Maastricht Acute Stress Test (MAST): A quick and non-invasive approach to elicit robust autonomic and glucocorticoid stress responses. *Psychoneuroendocrinology*. 2012;37(12):1998–2008.
7. Tustison NJ, Avants BB, Cook PA, Zheng Y, Egan A, Yushkevich PA, et al. N4ITK: improved N3 bias correction. *IEEE Trans Med Imaging*. 2010;29(6):1310–20.
8. Avants BB, Tustison N, Song G. Advanced normalization tools (ANTS). *Insight j*. 2009;2(365):1–35.
9. Zhang Y, Brady M, Smith S. Segmentation of brain MR images through a hidden Markov random field model and the expectation-maximization algorithm. *IEEE Trans Med Imaging*. 2001;20(1):45–57.
10. Dale AM, Fischl B, Sereno MI. Cortical surface-based analysis: I. Segmentation and surface reconstruction. *Neuroimage*. 1999;9(2):179–94.
11. Klein A, Ghosh SS, Bao FS, Giard J, Häme Y, Stavsky E, et al. Mindboggling morphometry of human brains. *PLoS Comput Biol*. 2017;13(2):e1005350.
12. Wang S, Peterson DJ, Gatenby JC, Li W, Grabowski TJ, Madhyastha TM. Evaluation of field map and nonlinear registration methods for correction of susceptibility artifacts in diffusion MRI. *Front*

- Neuroinform. 2017;11:17.
13. Huntenburg JM. Evaluating nonlinear coregistration of BOLD EPI and T1w images. Freie Universität Berlin; 2014.
  14. Treiber JM, White NS, Steed TC, Bartsch H, Holland D, Farid N, et al. Characterization and correction of geometric distortions in 814 diffusion weighted images. PLoS One. 2016;11(3):e0152472.
  15. Greve DN, Fischl B. Accurate and robust brain image alignment using boundary-based registration. Neuroimage. 2009;48(1):63–72.
  16. Jenkinson M, Smith S. A global optimisation method for robust affine registration of brain images. Med Image Anal. 2001;5(2):143–56.
  17. Cox RW, Hyde JS. Software tools for analysis and visualization of fMRI data. NMR Biomed An Int J Devoted to Dev Appl Magn Reson Vivo. 1997;10(4-5):171–8.
  18. Lanczos C. A precision approximation of the gamma function. J Soc Ind Appl Math Ser B Numer Anal. 1964;1(1):86–96.
  19. Pruim RHR, Mennes M, van Rooij D, Llera A, Buitelaar JK, Beckmann CF. ICA-AROMA: A robust ICA-based strategy for removing motion artifacts from fMRI data. Neuroimage. 2015;112:267–77.
  20. Stagg CJ, Wylezinska M, Matthews PM, Johansen-Berg H, Jezzard P, Rothwell JC, et al. Neurochemical Effects of Theta Burst Stimulation as Assessed by Magnetic Resonance Spectroscopy. J Neurophysiol. 2009;101(6):2872–7.
  21. Stagg CJ, Best JG, Stephenson MC, O’Shea J, Wylezinska M, Kincses ZT, et al. Polarity-sensitive modulation of cortical neurotransmitters by transcranial stimulation. J Neurosci. 2009;29(16):5202–6.
  22. Mescher M, Merkle H, Kirsch J, Garwood M, Gruetter R. Simultaneous in vivo spectral editing and water suppression. NMR Biomed. 1998;11(6):266–72.
  23. Mullins PG, McGonigle DJ, O’Gorman RL, Puts NAJ, Vidyasagar R, Evans CJ, et al. Current practice in the use of MEGA-PRESS spectroscopy for the detection of GABA. Neuroimage. 2014;86:43–52.
  24. Tremblay S, Beaulé V, Proulx S, Lafleur LP, Doyon J, Marjańska M, et al. The use of magnetic resonance spectroscopy as a tool for the measurement of bi-hemispheric transcranial electric

- stimulation effects on primary motor cortex metabolism. *J Vis Exp*. 2014;93.
25. Marjańska M, Lehericy S, Valabrègue R, Popa T, Worbe Y, Russo M, et al. Brain dynamic neurochemical changes in dystonic patients: A magnetic resonance spectroscopy study. *Mov Disord*. 2013;28(2):201–9.
  26. Duda JM, Moser AD, Zuo CS, Du F, Chen X, Perlo S, et al. Repeatability and reliability of GABA measurements with magnetic resonance spectroscopy in healthy young adults. *Magn Reson Med*. 2021;85(5):2359–69.
  27. Kreider RB, Kalman DS, Antonio J, Ziegenfuss TN, Wildman R, Collins R, et al. International Society of Sports Nutrition position stand: safety and efficacy of creatine supplementation in exercise, sport, and medicine. *J Int Soc Sports Nutr*. 2017;14(1):18.
  28. Turner CE, Russell BR, Gant N. Comparative quantification of dietary supplemented neural creatine concentrations with 1H-MRS peak fitting and basis spectrum methods. *Magn Reson Imaging*. 2015;33(9):1163–7.
  29. Geramita M, van der Veen JW, Barnett AS, Savostyanova AA, Shen J, Weinberger DR, et al. Reproducibility of prefrontal  $\gamma$ -aminobutyric acid measurements with J-edited spectroscopy. *NMR Biomed*. 2011;24(9):1089–98.
  30. Chen X, Fan X, Hu Y, Zuo C, Whitfield-Gabrieli S, Holt D, et al. Regional GABA concentrations modulate inter-network resting-state functional connectivity. *Cereb Cortex*. 2019;29(4):1607–18.
  31. Kim S-Y, Kaufman MJ, Cohen BM, Jensen JE, Coyle JT, Du F, et al. In vivo brain glycine and glutamate concentrations in patients with first-episode psychosis measured by echo time-averaged proton magnetic resonance spectroscopy at 4T. *Biol Psychiatry*. 2018;83(6):484–91.
  32. Pruessner JC, Dedovic K, Khalili-Mahani N, Engert V, Pruessner M, Buss C, et al. Deactivation of the limbic system during acute psychosocial stress: evidence from positron emission tomography and functional magnetic resonance imaging studies. *Biol Psychiatry*. 2008;63(2):234–40.
  33. Menon V. Large-scale brain networks and psychopathology: a unifying triple network model. *Trends Cogn Sci*. 2011;15(10):483–506.
  34. Qiu Y, Fan Z, Zhong M, Yang J, Wu K, Huiqing H, et al. Brain activation elicited by acute stress: An ALE meta-analysis. *Neurosci Biobehav Rev*. 2022;132:706–24.
  35. Smith SM, Fox PT, Miller KL, Glahn DC, Fox PM, Mackay CE, et al. Correspondence of the brain's functional architecture during activation and rest. *Proc Natl Acad Sci*. 2009;106(31):13040–5.

36. Beckmann CF, Mackay CE, Filippini N, Smith SM. Group comparison of resting-state FMRI data using multi-subject ICA and dual regression. *Neuroimage*. 2009;47(Suppl 1):S148.
37. Filippini N, MacIntosh BJ, Hough MG, Goodwin GM, Frisoni GB, Smith SM, et al. Distinct patterns of brain activity in young carriers of the APOE- $\epsilon$ 4 allele. *Proc Natl Acad Sci*. 2009;106(17):7209–14.
38. Smith SM, Miller KL, Salimi-Khorshidi G, Webster M, Beckmann CF, Nichols TE, et al. Network modelling methods for FMRI. *Neuroimage*. 2011;54(2):875–91.
39. Smith SM, Vidaurre D, Beckmann CF, Glasser MF, Jenkinson M, Miller KL, et al. Functional connectomics from resting-state fMRI. *Trends Cogn Sci*. 2013;17(12):666–82.
40. R Development Core Team. *R: A language and environment for statistical computing*. 2013.